De novo mutation hotspots in homologous protein domains identify function-altering mutations in neurodevelopmental disorders

Graphical abstract

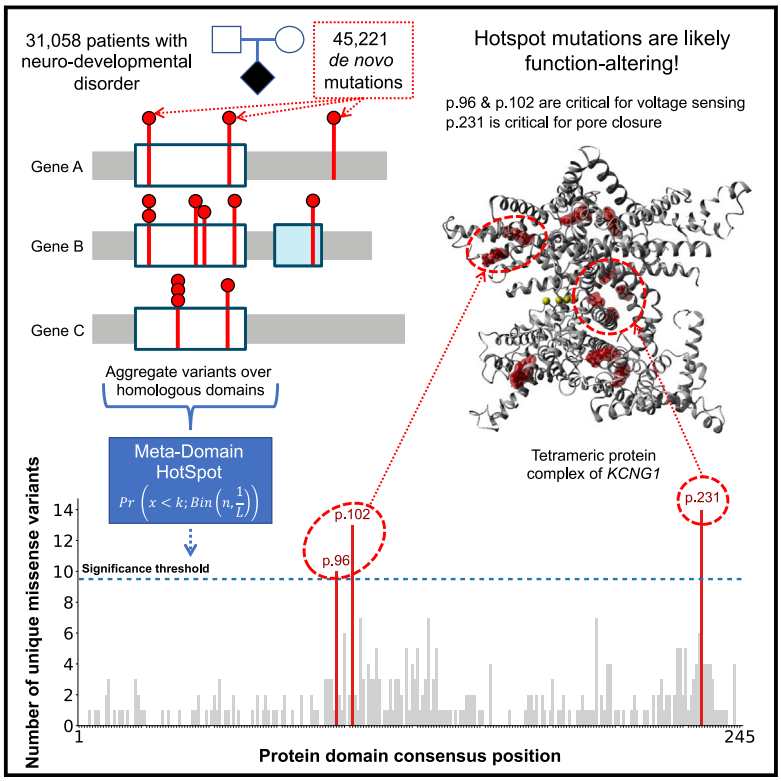

Authors

Laurens Wiel, Juliet E. Hampstead, Hanka Venselaar, ..., Gerrit Vriend, Joris A. Veltman, Christian Gilissen

Correspondence

christian.gilissen@radboudumc.nl

We developed MDHS which utilizes homologous protein domains to identify domain-based variant hotspots. Applying MDHS on *de novo* mutations from 31,058 patients with neurodevelopmental disorders (NDDs) identified three missense hotspots across 25 genes, of which 19 genes were previously associated with NDD. The identified missense mutations at the hotspots are suggested to alter function.

Wiel et al., 2023, The American Journal of Human Genetics *110*, 92–104
January 5, 2023
https://doi.org/10.1016/j.ajhg.2022.12.001

ARTICLE

De novo mutation hotspots in homologous protein domains identify function-altering mutations in neurodevelopmental disorders

Laurens Wiel,[1,2,6,7] Juliet E. Hampstead,[1,7] Hanka Venselaar,[2] Lisenka E.L.M. Vissers,[3] Han G. Brunner,[1] Rolph Pfundt,[3] Gerrit Vriend,[4] Joris A. Veltman,[5] and Christian Gilissen[1,*]

Summary

Variant interpretation remains a major challenge in medical genetics. We developed Meta-Domain HotSpot (MDHS) to identify mutational hotspots across homologous protein domains. We applied MDHS to a dataset of 45,221 *de novo* mutations (DNMs) from 31,058 individuals with neurodevelopmental disorders (NDDs) and identified three significantly enriched missense DNM hotspots in the ion transport protein domain family (PF00520). The 37 unique missense DNMs that drive enrichment affect 25 genes, 19 of which were previously associated with NDDs. 3D protein structure modeling supports the hypothesis of function-altering effects of these mutations. Hotspot genes have a unique expression pattern in tissue, and we used this pattern alongside *in silico* predictors and population constraint information to identify candidate NDD-associated genes. We also propose a lenient version of our method, which identifies 32 hotspot positions across 16 different protein domains. These positions are enriched for likely pathogenic variation in clinical databases and DNMs in other genetic disorders.

Introduction

The interpretation of sequence variation in the context of disease remains one of the biggest challenges in genetics. *De novo* mutations (DNMs) in protein-coding genes are an established cause of neurodevelopmental disorders (NDDs),[5] and roughly ~45% of NDDs are caused by a DNM in a protein-coding gene.[6,7] By modeling the probability of DNMs occurring in specific genes, one can identify genes that are enriched for DNMs in patient cohorts, provided that large-enough cohorts are available. This statistical identification of NDD-associated genes requires ever-larger collections of affected individuals.[1,7–10] A recent study of DNMs in 31,058 individuals with NDDs concluded that NDD-association of genes still is far from saturated and that over a thousand NDD-associated genes are still to be identified.[1]

Several studies of NDD-affected individuals have found that for specific genes, missense DNMs cluster in functional regions, and that this fact can be used to identify disease-associated genes.[1,11,12] Conserved protein domains are of particular interest, because they harbor ~71%[13] of all curated disease-causing missense variants in the Human Gene Mutation Database (HGMD)[14] and ClinVar.[15] Indeed, missense DNMs in NDD genes are almost three times more likely to be located in protein domains.[1] Clustered missense DNMs in these genes may act not through haploinsufficiency, but rather through dominant-negative or gain-of-function effects.[11,12] The detection of mutation clusters, or hotspots, can be a crucial step toward associating genes with NDDs[16] and for gaining insight into underlying disease mechanisms.[12]

Aggregation of variation across homologous domains can be a useful method to gain insight into patterns of variation[13,17,18] and can increase statistical power to detect mutation hotspots. Methods such as mCluster[19] and the DS-Score[20] have been developed to detect re-occurrence of missense mutations at equivalent positions in protein domains. However, these methods cannot robustly be applied to population datasets. Therefore, we developed Meta-Domain HotSpot (MDHS), a method to detect mutation clustering at evolutionary equivalent positions across homologous protein domains. We applied this method to DNMs from a large cohort of NDD-affected individuals to identify protein consensus positions enriched for missense variation.

Material and methods

Dataset of *de novo* mutations

We obtained the set of 45,221 DNMs from the Kaplanis et al. study.[1] These DNMs were identified in 31,058 DD-affected individuals combined across three centers. The genetic testing approach of these patients were described previously per center: DDD,[7]

[1]Department of Human Genetics, Radboud Institute for Molecular Life Sciences, Radboud University Medical Center, Nijmegen 6525 GA, the Netherlands; [2]Centre for Molecular and Biomolecular Informatics, Radboud Institute for Molecular Life Sciences, Radboud University Medical Center, Nijmegen 6525 GA, the Netherlands; [3]Department of Human Genetics, Donders Institute for Brain, Cognition and Behaviour, Radboud University Medical Center, Nijmegen 6525 GA, the Netherlands; [4]Baco Institute of Protein Science, Baco, 5201 Mindoro, Philippines; [5]Biosciences Institute, Faculty of Medical Sciences, Newcastle University, Newcastle upon Tyne NE1 3BZ, UK; [6]Department of Medicine, Division of Cardiovascular Medicine, School of Medicine, Stanford University, Stanford, CA, USA
[7]These authors contributed equally
*Correspondence: christian.gilissen@radboudumc.nl
https://doi.org/10.1016/j.ajhg.2022.12.001.

GeneDX,[21] and Radboudumc.[8] All individuals that underwent genetic testing provided informed consent.[1] Subsets of these patients have been analyzed and reported in previous publications.[7,21–23]

Developmental disorder diagnostic gene lists

We use the diagnostic lists of DD-associated genes from the Kaplanis et al. study. We consider all genes statistically associated with NDDs in this study to be NDD genes (novel, consensus, and discordant genes, total genes = 1,010).[1]

Additionally, we used the Deciphering Developmental Disorders Genotype2Phenotype (DDG2P, accessed 22-04-2021) list to assess the burden of function-altering mutational mechanisms already described in hotspot gene families. We considered activating, gain-of-function, dominant-negative, and increased gene dosage mutation consequences in this list to be function altering.

Annotation of transcript details, protein and meta-domain position annotation

The DNMs (Data S1) were annotated with corresponding GENCODE[24] transcripts from release 19 GRCh37.p13 Basic set, protein information from UniProtKB/Swiss-Prot[25] Release 2016_09, Pfam-A[26] v30.0 protein domains information, and meta-domain[13] positions using a local version of the MetaDome[17] web server (code available at https://github.com/cmbi/metadome). Meta-domains are multiple sequence alignments of regions within human protein-coding genes that correspond to Pfam protein domain families. The DNMs that correspond to Pfam consensus positions are annotated with the corresponding Pfam domain ID and consensus position.

Filtering the annotated DNMs

The annotation process can result in multiple GENCODE gene transcripts per DNM. To ensure a single GENCODE transcript per gene we performed a filtering step by the following order of criteria:

1. Filter to variants with transcript consequence: missense, synonymous, or stop-gained
2. The transcript corresponds to a human canonical or isoform entry in Swiss-Prot
3. This transcript contains all (or most) of the *de novo* mutations for the corresponding gene
4. The transcript translates to the longest protein sequence length
5. If multiple transcripts remain for a gene, one of these is selected
6. Filter variants only to those that are in a Pfam protein domain

MDHS: Detection of variant hotspots in homologous protein domains

The Pfam domain ID and consensus position allows for aggregation of genetic variants through meta-domain positions. To identify meta-domain positions that are significantly enriched with variants, we created the MDHS (Meta-Domain HotSpot) p value as follows:

$$\text{MDHS p value} = Pr\left(x < k;\ Bin\left(n, \frac{1}{L}\right)\right) \qquad \text{(Equation 1)}$$

In the context of meta-domains, n corresponds to the total number of aggregated genetic variants for the Pfam domain ID, L is the total number of possible consensus positions for a Pfam domain ID, k is the total number of genetic variants aggregated at a single consensus position, and $x = k - 1$, which depicts the chance of finding less than observed genetic variants at the consensus position. The MDHS p value is adapted from the mCluster[19] and DS-Score.[20] In line with these methods, variants are assumed to follow a binomial distribution. We correct the MDHS p value via the Bonferroni method for the total number of Pfam protein domain IDs considered. If a Bonferroni corrected MDHS p value < 0.05, we consider it to be a significant mutational hotspot.

Our code to analyze the MDHS p value was optimized to compute only for domains which can have significant hotspots. It implements a filter for domain families which works as follows: (1) Count the number of domain consensus positions with one or more variant as *n_hotspot_candidates*. (2) Count the number of DNMs that span at least more than one unique protein position at each consensus position and sum them up to represent *n_hotspots_with_variation_from_more_then_one_protein_position*. (3) Apply the filter criteria such that each domain family abides:

$$\frac{n\_hotspots\_with\_variation\_from\_more\_then\_one\_protein\_position}{n\_hotspot\_candidates} > 1$$

See the value in column "hotspot_uniqueness" in Data S2, S3, and S4.

Stringent and lenient counting of variants in MDHS

We use two ways to determine variable k in the MDHS p value (Equation 1). Unless otherwise specified, we count unique variants by considering mutated chromosomal positions only once, thereby reducing the impact of recurrent mutations in a single gene (stringent). Alternatively, we refer to a lenient way of variant counting when we count every mutation equally (including recurrent mutations). For a schematic, see Figure 1.

Functional characterization

We used the Ensembl Variant Effect Predictor (VEP)[27] to annotate all DNMs at hotspot sites (Data S5) with gnomAD allele frequency (AF),[28] SIFT,[29] Polyphen-2,[30] MPC,[31] and the CADD_Phred.[32] MetaDome[17] tolerance indication is a gene-based regional d_N/d_S based on gnomAD missense and synonymous mutation counts and was obtained manually. ACMG[33] classification was obtained through variant curation by a laboratory specialist. Available phenotype information for individuals with missense mutations in hotspot positions can be found in Data S6.

Protein 3D structure modeling of the genes with identified hotspots

For each of the 25 genes with a DNM located at one of the hotspots, we submitted the corresponding protein sequence (based on the transcript of Filtering the annotated DNMs) to the YASARA & WHAT IF Twinset[34,35] homology modeling script using the default settings. The regions corresponding to the PF00520 were extracted from all resulting homology structures and combined in a single YASARA scene and then structurally aligned using the MOTIF script. The structures are available in Data S7 and can be accessed through the freely available YASARA View software. The protein structure effects of mutations have been reported in Data S8.

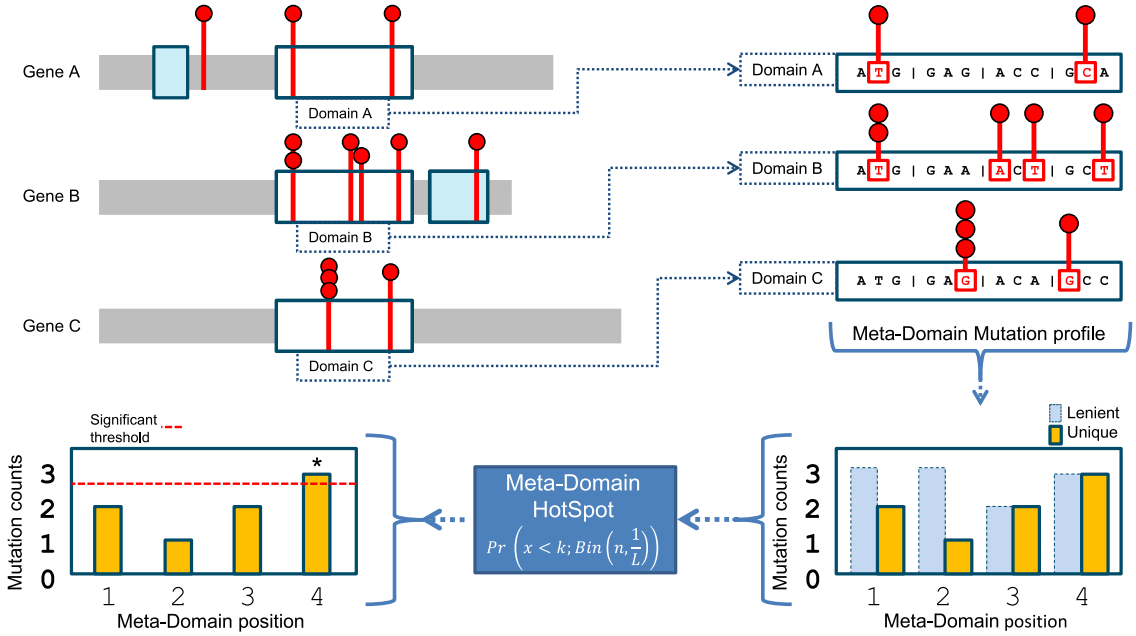

Figure 1. Workflow of how mutations are extracted from homologous domain regions within genes and aggregated to meta-domain positions

By clockwise orientation, starting in the upper left there are three protein representations of hypothetical genes A, B, and C with the mutations identified within a cohort are displayed as red lollipops, the domains as blue and white boxes. The white boxes represent domains that are homologous and are extracted and aligned, including their mutations, and displayed on the upper right part of this image as domains A, B, and C. The mutations within a codon are then aggregated over corresponding homologous domain positions based on sequence alignments to form a meta-domain mutation profile (bottom right). Here, the recurring mutations are counted only once for unique counts (for stringent hotspot identification). The unique counts are the input for variable k to compute a positional MDHS p value (Equation 1). Together with the total number of mutations n in the meta-domain mutation profile, the significance threshold (red dotted line left bottom) can be determined which indicates a meta-domain hotspot if the mutational count exceeds it.

Population constraint

Constraint information, including observed and expected counts, z-scores, and pLI, pNull, and pRec were calculated on gnomAD v.2.1.1.[28]

Regional missense constraint

Genes with regions of differential missense constraint were identified as described by Samocha et al.[31] in the ExAC[36] dataset. In brief, the fraction of observed missense variation along a transcript was tested for uniformity using a likelihood ratio test. If the distribution was not uniform, the transcript was considered to have evidence of regional missense constraint. 2,700 genes showed evidence of at least two regions of distinct missense constraint using this method.

Expression data

Pre-computed tissue expression values in transcripts per million (TPM) were taken from GTEx v.8 (GTEx_Analysis_2017-06-05_v8_RNASeQCv1.1.9_gene_median_tpm.gct.gz).[37,38]

Gene sets for constraint and expression analysis

The set of 56,200 genes for which median TPM values were available was divided into four sets: proposed novel hotspot genes, hotspot genes, NDD-associated genes, and control genes. Genes containing a mutation hotspot were divided into two categories: hotspot genes (n = 19) and proposed novel hotspot genes (n = 6). These categories were distinguished by their presence on the DD gene list (see Developmental disorder diagnostic gene lists); hotspot genes are on this list while proposed novel hotspot genes are not. The remaining genes were divided into NDD-associated genes (n = 992, excluding hotspot genes) and control genes not statistically associated with intellectual disability or developmental delay (n = 55,183). For some analyses, control genes present in DDG2P (n = 1,250, accessed 22-04-2021) or OMIM (n = 3,402, accessed 31-08-2021) but not statistically associated with NDDs were considered separate classes. Additionally, only some of these genes had population constraint information available from gnomAD v.2.1.1 (n = 19,658). Genes in all sets can be found in Data S9.

Of the 56,200 genes described above, 105 contained a PF00520 domain in MetaDome v.1.0.1. These 105 genes represented 19 hotspot genes, 6 proposed novel hotspot genes, 12 NDD-associated genes not containing a missense DNM at a hotspot position in our cohort, and 68 control genes (of which 6 are present in DDG2P and 26 in OMIM; Data S10).

Proportion of expressed genes across GTEx tissues

A fixed level of TPM > 1 was used to define expression in each tissue. NDD-associated and control genes were randomly sampled 1,000 times into sets of 19 genes, and the proportion of expressed genes (number of genes with TPM > 1/total number of genes) was calculated for each set. This generated a distribution of proportions across 54 GTEx tissues. The proportion of expressed hotspot genes per tissue was computed without sampling.

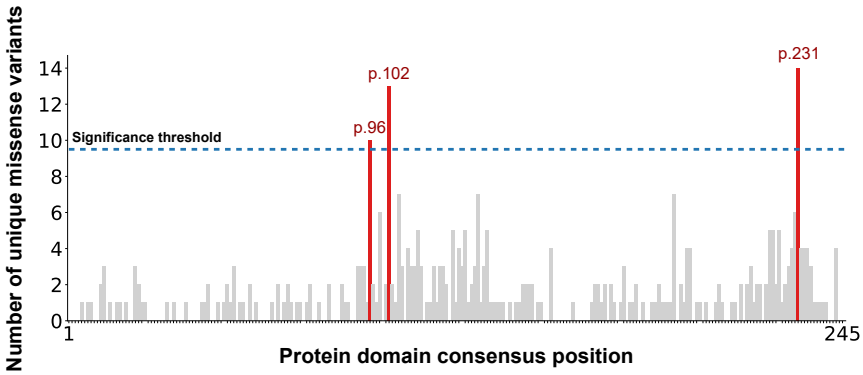

Figure 2. The count distribution of missense DNMs aggregated over the ion transport protein domain family (PF00520)
The total consensus length of this domain is 245 and the sum of the count distribution is 350. The significance threshold is displayed as a dotted black line, computed via the MDHS (Equation 1). The bars that exceeded the significance threshold are colored in red and represent the mutational hotspots p.96, p.102, and p.231.

TPM differences between tissue groups

In order to assess expression differences between brain and other tissues, GTEx tissues were divided into two groups. We considered the amygdala, anterior cingulate cortex (BA24), caudate (basal ganglia), cerebellar hemisphere, cerebellum, cortex, frontal cortex (BA9), hippocampus, hypothalamus, nucleus accumbens (basal ganglia), putamen (basal ganglia), spinal cord (cervical c-1), and substantia nigra brain tissues (n = 12). All non-brain tissues were included in the "other tissues" set (n = 42). The TPM value for each tissue set was defined as the median TPM of all tissues in the set. Based on these differences, we modeled the brain TPM distribution in hotspot genes and control genes and the other tissue TPM distribution in hotspot genes and NDD-associated genes as normal distributions. For each set of distributions, a likelihood ratio of belonging to each distribution was calculated. Proposed novel hotspot genes were considered to have evidence for association with NDDs if they were more likely to belong to the hotspot gene distribution across both tests.

Filtering and annotation of additional *de novo* mutation cohorts

We analyzed the enrichment of missense and synonymous DNMs in lenient hotspot positions across a total of three additional published DNM cohorts. We used an autism-spectrum disorder (ASD) cohort published by Satterstrom et al.[2] (35,584 total individuals, 11,986 with ASD), a congenital heart defect (CHD) cohort published by Jin et al.[3] (2,645 trios), and a cohort of healthy individuals sequenced by Jonsson et al.[4] (1,548 trios). To increase our power to find significant differences at lenient hotspot positions, we pooled the Jonsson et al.[4] healthy individuals with unaffected siblings from the Satterstrom et al.[3] ASD cohort (1,740 siblings) for a total of 3,288 unaffected individuals.

Annotation of meta-domain protein consensus positions for these datasets was done as previously described for Kaplanis et al.[1] using MetaDome. The number of PTV, missense, and synonymous SNVs in Pfam protein domains in each dataset can be found in Table S1.

Variant annotation

Variants at protein consensus positions were checked for clinical interpretation across four curated variant databases: ClinVar, HGMDPro, Swiss-Prot, and VKGL, all accessed 21-08-2021. Mapping of protein consensus positions to GRCh37 genomic positions for each gene was done using MetaDome.

For analysis on stringent hotspot positions, ClinVar data were unfiltered on evidence level or review status. We classified missense variation as LP (pathogenic or likely pathogenic, ACMG Class V or IV) or VUS (variant of uncertain significance, ACMG Class III) based on the most severe class across all four databases (Data S6).

For the enrichment analysis on lenient hotspot positions, only ClinVar and VKGL data were used because these two databases include likely benign variants. ClinVar data were filtered on review status (required to be one of "practice guideline," "reviewed by expert panel," "criteria provided, multiple submitters, no conflicts," "criteria provided, single submitter"). Variants were classified as LP (ACMG class V or IV), VUS (ACMG class III), or LB (benign or likely benign, ACMG class II or I). Variants with conflicting interpretations of pathogenicity within or between databases (LP and LB annotations) were removed, as were variants with only VUS annotations.

Results

General description of the data and the processing steps

To identify hotspots of *de novo* mutations in homologous protein domains, we computed MDHS (Equation 1) based on unique DNMs in NDD-affected individuals (Figure 1). These unique DNMs are aggregated over homologous protein domains to form a domain-based variation profile or a "meta-domain."[13] Next, MDHS assigns a p value to each position, in each meta-domain, based on how closely that position's aggregated DNMs abide a binomial distribution in perspective of the entire meta-domain (material and methods). This was done for each variant type separately (missense, synonymous, nonsense). We first mapped 45,221 DNMs resulting from 31,058 individuals with developmental disorders[1] onto gene transcripts using MetaDome[17] (material and methods). Then, we aggregated these to 12,389 meta-domain[13] positions (Data S1). The final 15,322 DNMs represent 73.7% missense (n = 11,288), 21.1% synonymous (n = 3,229), and 5.3% stop-gained mutations (n = 805) (Table S2).

Stringent DNM hotspots identified using MDHS

We initially used a stringent approach where recurrent DNMs were counted only once to prevent hotspots driven by DNMs in a single gene. Using all 11,288 missense DNMs in 2,032 protein domain families, our method identified three significant hotspots (Data S2 and S5) comprising 37 unique missense DNMs (57 total) in 25 different genes (Data S2, Table S3). Strikingly, all three hotspots are in domains belonging to the ion transport protein domain family (PF00520) (Figure 2). As a sanity check and to validate our

Table 1. Overview of the genes with missense variants at hotspot positions together with evidence of candidate association to DDs

Gene	Variant	Functional NDD association	gnomAD AF/ SIFT/Polyphen-2/ MPC/CADD/ MetaDome score	DNMs in other NDD-associated genes	Clinical interpretation[a]
TRPM5 (MIM: 604600)	*NC_000011.9:g.2432929C>T; ENST00000452833:c.2549G>A; p.Arg850Gln; PF00520:p.102*	unknown	1.20E−02//deleterious (0)// probably damaging (1)//-// 28.7//intolerant (0.49)	2: *SLC9A1* *ADNP*	uncertain (class 3)
TPCN2 (MIM: 612163)	*ENST00000294309:c.1633C>A; p.Arg545Ser; PF00520:p.96*	part of the mTOR complex[39]	-//deleterious (0.02)// probably damaging (0.965)//0.80//23.5// slightly intolerant (0.67)	0	–
TPCN1 (MIM: 609666)	*ENST00000550785:c.794G>A; p.Arg265Gln; PF00520:p.96*	part of the mTOR complex[39]	7.97E−06//tolerated (0.1)// possibly damaging (0.903)// 2.35//26.1//tolerant (1.03)	0	likely benign (class 2)
KCNH5 (MIM: 605716)	*ENST00000322893:c.980G>A; p.Arg327His; PF00520:p.102*	identical VUS (p.327R>H) in unrelated individual with epileptic encephalopathy[40]	-//deleterious (0)// probably damaging (0.999)//1.93//32// intolerant (0.19)	0	–
KCNG1 (MIM: 603788)	*ENST00000371571:c.1046G>A; p.Arg349His; PF00520:p.102*	involved in neuronal differentiation[41]	-//deleterious (0)// probably damaging (1)//2.74//32//highly intolerant (0.13)	0	–
CACNA1B (MIM: 601012)	*NC_000009.12:g.137984223G>A; ENST00000371372:c.1742G>A; p.Arg581His; PF00520:p.102*	nonsense DNMs in *CACNA1B* lead to an NDD with seizures and nonepileptic hyperkinetic movements (MIM: 618497)[42]	4.58E−03//deleterious (0)//probably damaging (0.999)//1.32//26.1// highly intolerant (0.13)	0	–

Missense variants in these genes have previously not been associated with NDDs. First column indicates the gene and OMIM identifier. Second column indicates the identified DNM at the hotspot position. Third column indicates a previously described functional association of the gene or variant to NDD. Fourth column indicates different prediction scores of variant pathogenicity, the fifth indicates if the same individual has any DNMs located in known NDD-associated genes, and sixth column is ACMG classification. The last three rows (*KCNH5*, *KCNG1*, and *CACNA1B*) are novel candidate NDD genes based on additional evidence as described in this paper. Evidence for ACMG classification is provided in Table S12. Genomic positions and additional phenotype information for all variants where available can be found in Data S6 and S17.

[a]Variants were clinically interpreted where proband phenotype information was available (see Data S6).

approach, we also performed the stringent method separately for the 3,229 synonymous and 805 stop-gained DNMs in our cohort and identified no significant hotspots (Data S3 and S4).

The three significant missense hotspots we identify are located on domain consensus positions p.96 (10 unique DNMs, $p = 3.6 \times 10^{-2}$), p.102 (13 unique DNMs, $p = 7.1 \times 10^{-5}$), and p.231 (14 unique DNMs, $p = 7.5 \times 10^{-6}$) of the ion transport domain family. The ion transport protein domain family is one of four protein domain families that we previously found to be significantly enriched with missense DNMs in NDD-associated genes.[1] Specifically, this Pfam domain family consists of sodium, potassium, and calcium ion channels and has six transmembrane helices in which the last two helices determine ion selectivity. Of the 25 genes identified with a missense DNM at a hotspot, 19 are known NDD-associated genes, or hotspot genes, representing a 3.17-fold enrichment of known NDD-associated genes ($p = 1.11 \times 10^{-13}$ chi-square test, Table S4). The remaining 6 genes, proposed novel hotspot genes, have not yet been associated with NDDs (Table 1).

Effects of missense mutations at stringent hotspots on protein structure

Mutations that cluster in genes have previously been associated with likely function-altering effects.[12] We find that 6 out of 16 hotspot genes present in the Developmental Disorder Genotype2Phenotype (DDG2P) gene list are known to have an activating or gain-of-function mutation consequence ($p = 0.0008$, Fisher's exact test), underscoring that missense mutations at hotspot positions are likely function altering (Table S5). To further investigate this, we created 3D protein structure homology models for each of the 25 genes (Data S7, material and methods). Ion transport protein domain 3D structures are 3-fold more identical to each other in conformation than their protein sequences would suggest (CATH-Gene3D ID: 1.20.120.350).[43] This structural overlap encouraged us to investigate whether molecular effects of missense variants at these hotspots are likely to have similar impact on domain function across the 25 genes (Data S8).

In the 25 homology models, we find that hotspot p.96 (Figure 3A) and p.102 (Figure 3B) are part of the voltage-sensing helix that is important for the channel

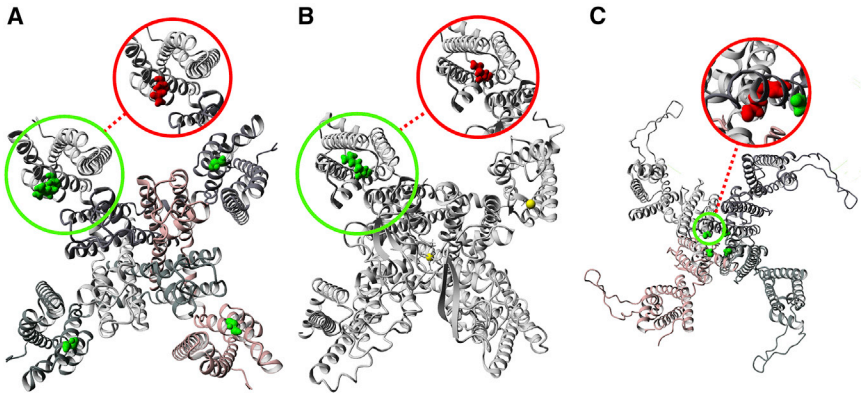

Figure 3. Changes in structure caused by missense DNMs in NDD-associated genes for each hotspot

(A) Homology model of the KCNQ3 (MIM: 602232) complex with missense DNM ENST00000388996:c.680G>A (p.Arg227Gln) marked as a green to red change. The KCNQ3 complex is a tetramer constructed from four copies of the KCNQ3 monomer. All monomers are marked in different color shades. This DNM is located at identified hotspot p.96. The wild-type arginine residue is part of the voltage-sensing helix and changed into a glutamine. This change causes it to lose the positive charged that was previously found to cause a function-altering mechanism of disease.[45]

(B) Homology model of CACNA1A (MIM: 601011) with missense DNM ENST00000360228:c.4988G>A (p.Arg1663Gln) marked as a green to red change. This DNM is located at identified hotspot p.102. The wild-type arginine residue is part of the voltage-sensing helix and changed into a glutamine. This change causes it to lose the positive charge that was previously found to cause a function-altering mechanism of disease.[46]

(C) Homology model of the KCNH1 (MIM: 603305) complex with missense DNM ENST00000271751:c.1486G>A (p.Gly496Arg) marked as a green to red change. The KCNH1 complex is a tetramer constructed from four copies of the KCNH1 monomer. All monomers are marked in different color shades. This DNM is located at identified hotspot p.231. The wild-type glycine residue is near the pore-closing region and changed into a much larger arginine. This may impact pore closure and was previously reported to result into a function-altering mechanism of disease.[47]

(in-)activation.[44] These results are in line with functional studies that have been performed for missense mutations at two of these hotspots.[45,46] Hotspot p.231 (Figure 3C) is part of the channel gate at the end of a transmembrane helix (Data S8). In addition, we find that missense mutations follow a specific pattern for each of these hotspots. Of the 13/16 missense DNMs located at hotspot p.96 and 20/20 at p.102 change the positively charged wild-type residue to lose the positive charge. Losing positive charges at these locations has previously been described to trigger a function altering disease-mechanism (Figures 3A and 3B).[45,46] At hotspot p.231, 20/21 of the missense DNMs changes the wild-type residue from a small into a larger residue. This change in residue size likely impacts the pore closure. This hypothesis is shared by Kortüm et al. who suggest this likely causes a steric hindrance and result into a function-altering mechanism of disease (Figure 3C).[47] Lastly, all hotspots are located at the surface of the protein structure, a feat that was previously observed to be characteristic for clustered missense DNMs in NDDs that likely act through non-haploinsufficiency.[12] Overall, this shows that missense mutations at the identified hotspots are likely deleterious to domain function.

Stringent hotspot genes are constrained against missense and loss of function variation

Dominant NDD genes are characterized by population constraint against damaging genetic variation.[23,28] We compared observed counts of loss of function, missense, and synonymous variants in control, NDD-associated, hotspot, and proposed novel hotspot genes in gnomAD v.2 to expected counts based on a null mutational model.[31] Both hotspot and novel hotspot genes are constrained against loss-of-function and missense variation (Figure 4A). Novel hotspot genes have lower constraint against loss-of-function variation than hotspot genes (Data S11). We also considered whether hotspots were located in regions of particular constraint against missense variation within genes. In total, 2,700 genes have statistical evidence of regional differences in missense constraint.[31] Of these, 16 are hotspot genes, representing a significant enrichment compared to control genes (Fisher exact test $p < 2.2 \times 10^{-16}$) and NDD-associated genes (Fisher exact test $p = 0.02$, Figure S1). Three are proposed novel hotspot genes (*KCNH5* [MIM: 605716], *CACNA1B* [MIM: 601012], *TPCN1* [MIM: 609666]). Using regional missense constraint information, we show that PF00520 domains in hotspot genes are significantly more constrained against missense variation than PF00520 domains in control genes ($p = 1.4 \times 10^{-7}$, Wilcoxon rank-sum test; Figure 4B), but similarly constrained compared to NDD-associated genes without a hotspot that also contain a PF00520 domain ($p = 0.65$, Wilcoxon rank-sum test).

Brain-specific expression of stringent hotspot genes

We analyzed the expression of the 19 known hotspot genes in approximately 948 donors across 54 tissues from the GTEx v8 release.[37] We observed that NDD genes and control genes have distinct gene expression patterns, with a higher proportion of NDD genes constitutively expressed across all tissues ($p < 2.2 \times 10^{-16}$, Fisher exact test; Table S6). Hotspot genes share a characteristic expression pattern compared to these two groups (Figure 5A), with a significantly higher proportion of hotspot genes expressed in the brain compared to control genes and significantly lower proportion expressed in all other tissues compared to NDD genes (in 40/42 non-brain tissues, Data S12). Given this tissue-specific expression pattern, we grouped GTEx tissues into two

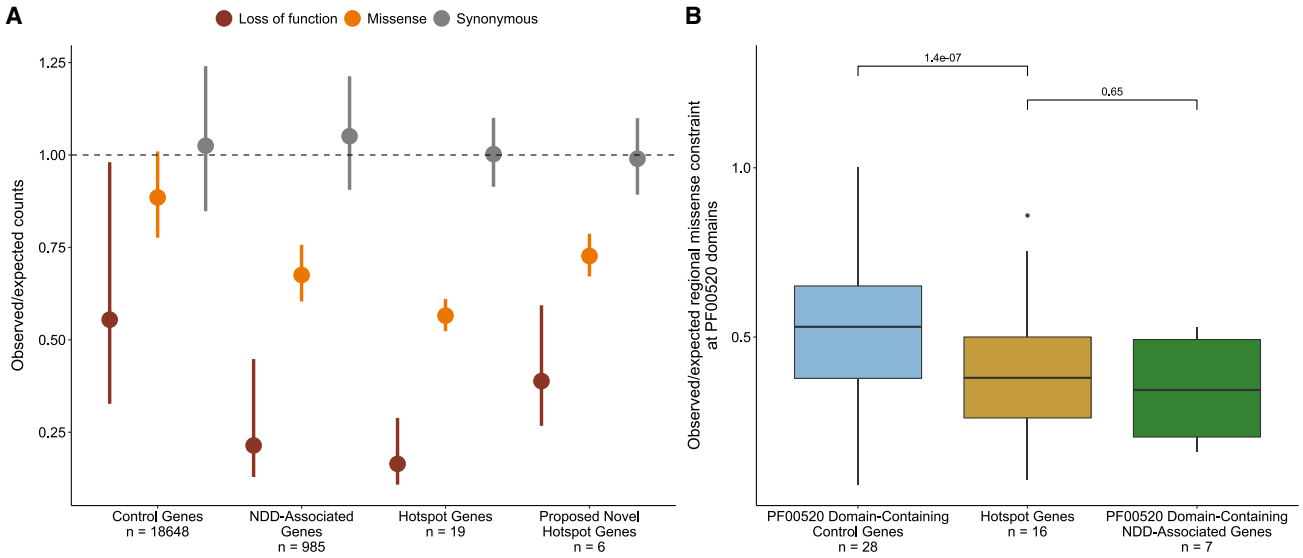

Figure 4. Hotspot genes are constrained against loss-of-function and missense variation

(A) Constraint in hotspot and proposed novel hotspot genes. The observed variant counts for loss of function (red), missense (orange), and synonymous (pink) variants from the gnomAD v.2 release were compared to the expected counts based on a null mutational model.[31] Points represent the mean observed/expected ratios for all genes in each set and bars denote the mean upper and lower bound fractions for these ratios. The dashed line at observed/expected = 1 indicates perfect adherence to the null mutational model (observed counts = expected counts); values that fall below this line are constrained.

(B) Mutation hotspots occur in missense constrained regions within genes. Regional missense constraint was compared across PF00520 domain-containing control genes (blue), PF00520 domain-containing NDD-associated genes (green), and hotspot genes (yellow). Boxes represent the lower and upper quartiles of the distribution, and whiskers represent the distance from 1.5× the interquartile range to the lower/upper quartiles.

tissue groups (brain and other tissues, material and methods). The hotspot gene set is significantly enriched for genes with higher expression in brain compared to control genes (89.4% versus 19.8% expressed higher in brain, $p = 2.985 \times 10^{-5}$, Fisher exact test) and NDD genes (89.4% versus 31.3%, $p = 0.002$, Fisher exact test) (Figure S2). Only two hotspot genes do not have higher expression in brain: *SCN10A* (MIM: 604427), which is constitutively unexpressed across tissues in GTEx samples, and *CACNA1C* (MIM: 114205) (median TPM in brain = 2.94, median TPM in other tissues = 4.35). We further show that this expression pattern is not characteristic of all genes containing an ion transport domain, but only the subset of these genes statistically associated with NDDs (Data S13, Figures S3 and S4).

We also compared the TPM distribution in brain and other tissues for control genes, NDD-associated genes, hotspot genes, and the six proposed novel hotspot genes (material and methods; Figure 5B). Both hotspot and NDD-associated genes had significantly higher TPM in brain tissues than control genes ($p = 0.0039$ and $p < 2.2 \times 10^{-16}$, Wilcoxon rank-sum test), and both hotspot genes and control genes had significantly lower TPM in other tissues than NDD-associated genes ($p < 2.2 \times 10^{-16}$ and $p = 2.08 \times 10^{-8}$, Wilcoxon rank-sum test; Figure S5). Modeling suggests that *CACNA1B* and *KCNG1* (MIM: 603788) belong to the hotspot gene distribution by odds ratio (Data S14). Additionally, we find 6 NDD-associated PF00520 domain-containing genes (*HCN1* [MIM: 602780], *TRPV3* [MIM: 607066], *KCNQ5* [MIM: 607357], *KCNC1* [MIM: 176258], *KCNC3* [MIM: 176264], *TRPM3* [MIM: 608961]) that also belong to the hotspot gene distribution by odds ratio. We hypothesize that missense mutations at hotspot positions in these six genes may also cause NDDs.

Missense mutations at lenient DNM hotspots are enriched in clinical databases

We also implemented a lenient version of MDHS that counts all missense variants at protein consensus positions, even if they recur between individuals (see material and methods, Figure S6). Counting recurrent missense variants gives us more power to detect hotspot positions, but these hotspot positions may be driven by missense variation in a single domain. Applying this lenient method to our cohort identified 32 significant missense hotspots across 16 Pfam protein domain families (Data S2 and S15) and no significant hotspots for synonymous or nonsense mutations (Data S3 and S4). 12 protein domain families had hotspots spanning multiple gene-codons based on 245 DNMs from 67 genes. 48 of these 67 genes (72%) are statistically associated with NDDs, representing a 2.53-fold enrichment ($p = 1.26^{-31}$ chi-square test; Table S7) and showing the merit of this approach. We find a significant enrichment of genes statistically associated with NDD (Fisher's exact $p < 2.2 \times 10^{-16}$) and DDG2P (Fisher's exact $p < 2.2 \times 10^{-16}$) genes at lenient hotspot positions (Figure S7).

We also find that missense variants at these positions are significantly more likely to be pathogenic or likely

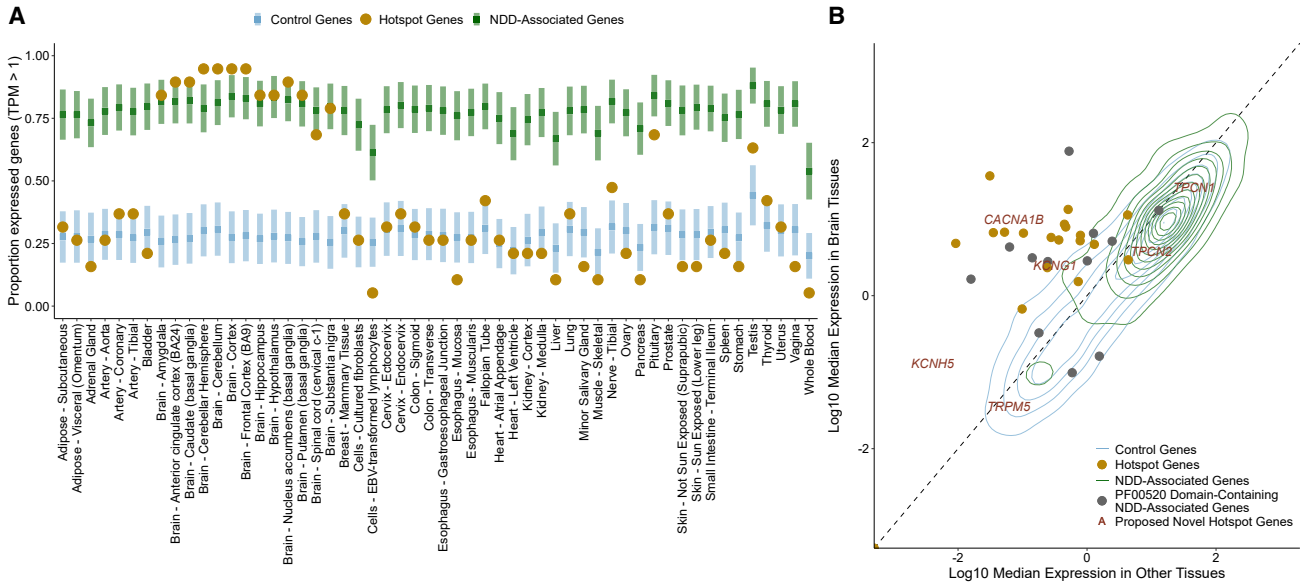

Figure 5. Hotspot genes have a distinct gene expression pattern

(A) Tissue expression of hotspot genes compared to control and other NDD genes. Expression of the 19 established NDD genes containing missense DNM(s) at a stringent mutation hotspots (hotspot genes, yellow) were evaluated across 54 GTEx tissues (x axis). Hotspot gene expression was compared to NDD genes (green) and control genes (blue). The y axis depicts the proportion of expressed genes (material and methods). Squares and bars depict the median and SD, respectively, of NDD and control gene distributions.

(B) TPM distribution in brain and other tissues varies across gene sets. Control (blue) and NDD-associated (green) genes are represented by 2D density distributions. Hotspot genes (yellow) are shown as points, as are NDD-associated genes containing a PF00520 domain (gray). Proposed novel hotspot genes are marked by their gene name in red text.

pathogenic in clinical databases (VKGL, Figure 6A; ClinVar, Figure 6B). We compared the proportion of reported likely pathogenic (LP) missense variants at hotspot positions to those at other protein consensus positions across the 16 Pfam domain families with a lenient hotspot (Figures 6A and 6B). We find a significant enrichment of LP variants at hotspot positions when we consider all positions (Fisher's exact $p < 2.2 \times 10^{-16}$, ClinVar; $p < 2.2 \times 10^{-16}$, VKGL), only positions without a DNM in our cohort (Fisher's exact $p < 2.2 \times 10^{-16}$, ClinVar; $p < 2.2 \times 10^{-16}$, VKGL), and only codons without a DNM in our cohort (Fisher's exact $p < 2.2 \times 10^{-16}$, ClinVar; $p = 3.08 \times 10^{-13}$, VKGL; Table S8).

Lenient hotspots are enriched for missense variation in autism-spectrum disorders

We investigated whether we could find further evidence for the identified lenient hotspots in a combined cohort of publicly available *de novo* mutation datasets for autism-spectrum disorders (ASD; 11,986 ASD probands, 35,584 individuals) and congenital heart defects (CHD; 2,654 trios) alongside DNMs from unaffected individuals (1,740 ASD siblings, 1,548 population control subjects; see material and methods).

We observe a significant enrichment of missense DNMs at hotspot positions in NDD and ASD cohorts compared to unaffected individuals (Fisher's exact $p = 3.5 \times 10^{-13}$, NDD; Fisher's exact $p = 0.007$, ASD; Fisher's exact $p = 0.07$, CHD; Figure 7A, Table S9). We observe no significant enrichment in synonymous DNMs at hotspot positions in any cohort (Table S10). However, we predict that some lenient hotspot positions are driven by mutational processes or ascertainment bias in particular genes and not necessarily by the cumulative effect of pathogenic mutations across several genes. To correct for this, we also tested for an enrichment of missense variants unique to ASD and CHD probands at lenient hotspots (Figure 7B, Table S11). We find a significant enrichment of these unique missense variants in ASD probands (Fisher's exact $p = 0.047$) but not in CHD probands (Fisher's exact $p = 1$). The majority (10/13, 77%) of the missense variants driving this enrichment in ASD probands are in genes statistically associated with NDDs.[1]

Discussion

By exploiting homology within the human genome, we were able to identify mutational clustering of DNMs at evolutionarily conserved positions across genes that share protein domains. We identify three stringent (p.96, p.102, p.231) and 32 lenient mutational hotspots across 16 Pfam domain families using our MDHS method. Missense DNMs at stringent hotspots are located in 25 genes within our cohort. Structural and functional work by us and others suggest that missense mutations at these positions may be function altering.[48,49] Functional work for hotspots in each of the 25 genes would be necessary to confirm this.

The hotspots we statistically identify in our cohort may have broader clinical relevance. We hypothesize that the

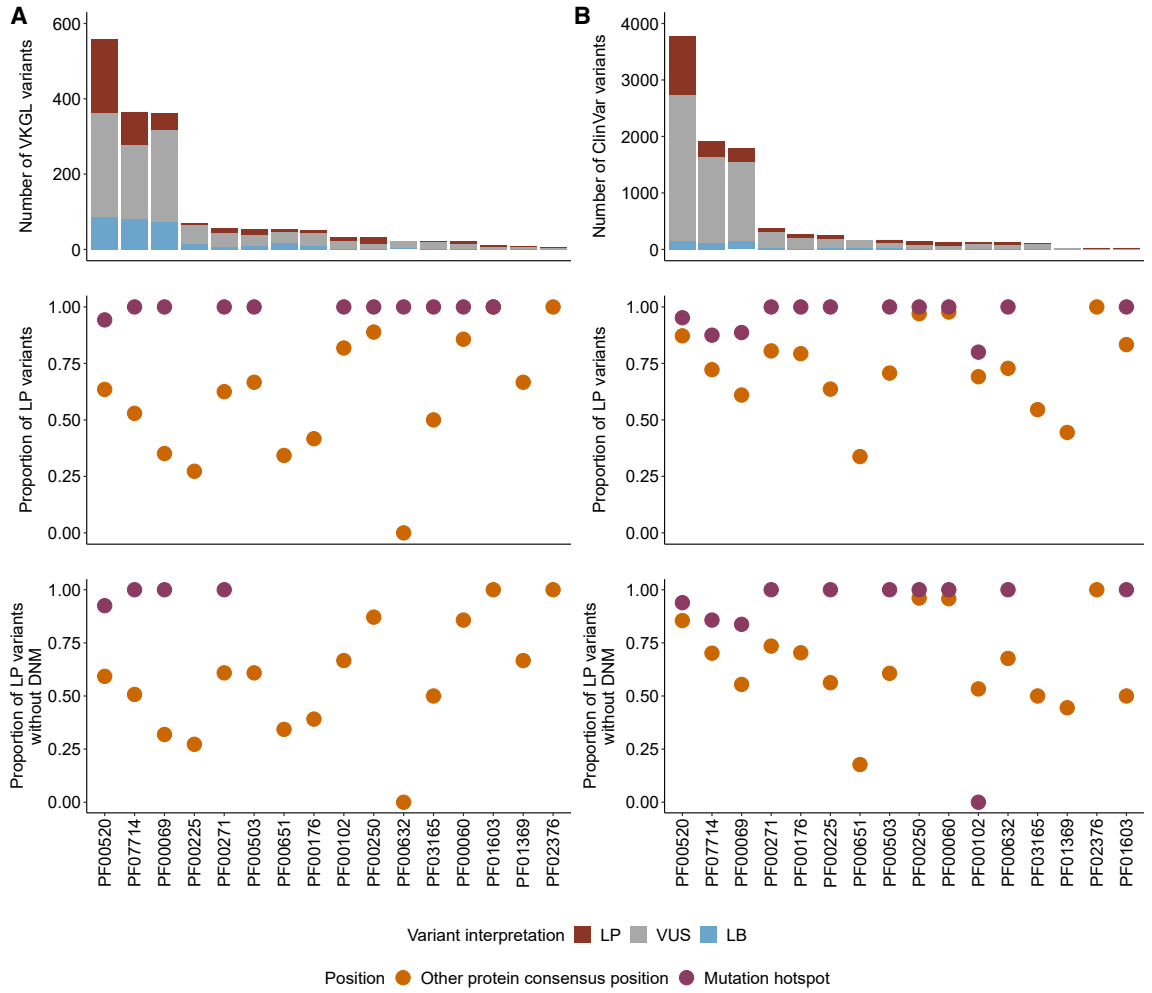

Figure 6. Lenient hotspots are enriched for likely pathogenic missense variation in clinical databases
Counts of likely pathogenic (LP, red), uncertain (VUS, gray), and likely benign (LB, blue) missense variants in VKGL (A) and ClinVar (B) in domains containing a lenient hotspot position. The proportion of LP missense variants (LP/(LP + LB), see material and methods) was compared between mutation hotspots (purple) and all other protein consensus positions within the domain (orange). This comparison was done for all possible missense variants in these domains (row 2) and with positions containing DNMs in our cohort excluded (row 3).

19 hotspot genes are examples of a broader class of ion transport domain-containing genes and that missense mutations at hotspot positions in these genes are generally damaging. Our finding that clinical databases contain many pathogenic missense mutations at hotspot positions in other monogenic disease genes (Data S16) supports this hypothesis. Other studies have shown that missense mutations in ion transport domain-containing genes may have position-specific functional effects.[50,51] Several of these mutations occur in genes not statistically associated with NDDs, indicating that missense mutations at hotspot positions could be pathogenic across a variety of disorders. In line with this, we observe that some PF00520 domain-containing NDD-associated genes have lower expression in brain but have a similar level of tissue-specific expression in a non-brain tissue. *SCN4A* (MIM: 603967), for example, is not expressed in brain and is predominantly expressed in skeletal muscle. Although the expression pattern of *SCN4A* is different from the hotspot genes presented in our analysis, hotspot positions in *SCN4A* are similarly constrained against missense variation (Figure 5B). We hypothesize that phenotypes associated with pathogenic mutations at hotspot positions may vary depending on where the mutated gene is expressed. For example, of the four PF00520 domain-containing genes predominantly expressed in skeletal muscle (*SCN4A, CACNA1S* [MIM: 114208], *RYR1* [MIM: 180901], and *KCNA7* [MIM: 176268]), three of these (*SCN4A, RYR1,* and *CACNA1S*) have pathogenic missense variation at hotspot positions in clinical databases (Data S16). Individuals with these mutations present with disorders of the skeletal muscle, including myotonia (MIM: 608390), paramyotonia (MIM: 168300), and hyperkalemic paralysis (MIM: 170500). Our work suggests that missense mutations at hotspot positions in *KCNA7* may also result in skeletal muscle disorders based on the tissue expression of *KCNA7* and the conservation of hotspot positions in the PF00520 domain of this gene.

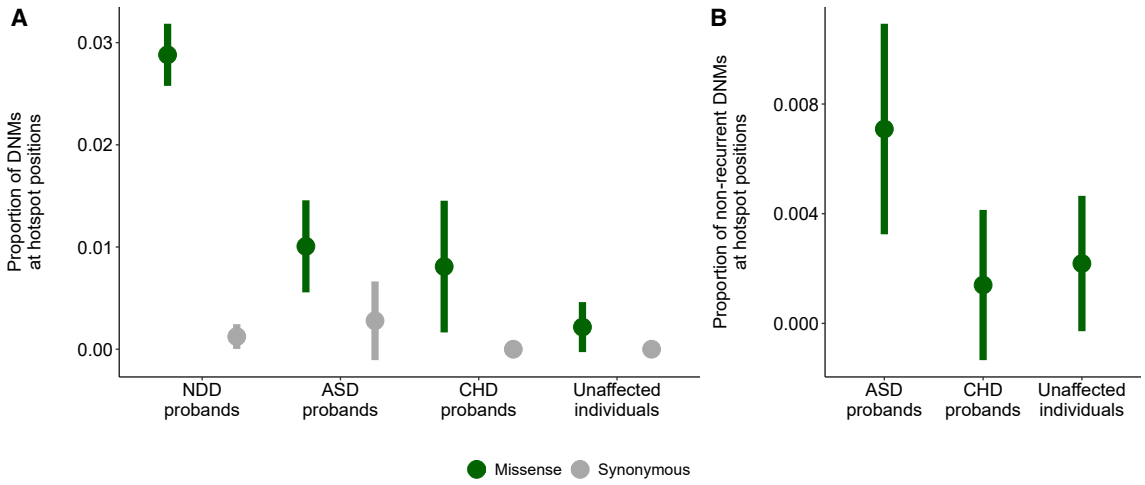

Figure 7. Affected individuals are enriched for missense variants in lenient hotspot positions compared to healthy population control subjects

(A) NDD and ASD are enriched for missense DNMs in lenient hotspot positions compared to unaffected individuals (green) but are not enriched for synonymous DNMs (gray). Only DNMs within protein consensus positions were used for this comparison (see material and methods).

(B) ASD probands are enriched for missense DNMs in lenient hotspot positions (green) not present in our NDD cohort.

Our method also identified six genes with a mutation at the hotspot location that have not previously been associated with NDDs. Three genes—*KCNH5, CACNA1B,* and *KCNG1*—have evidence supporting NDD association (Table 1). In *KCNH5,* the same DNM was described as a variant of unknown significance (VUS) in an individual with an epileptic encephalopathy,[40] and very recently a study of a cohort of NDD-affected individuals with *KCNH5* DNMs was published, including nine individuals with recurrent p.Arg327His mutations.[52] *CACNA1B* was recently established as an NDD-associated gene on the basis of LoF DNM enrichment.[42] In line with this, *CACNA1B* is the only proposed novel hotspot gene that is predicted to be intolerant to heterozygous loss of function by population constraint (pLI = 1; Data S11). However, our work suggests that the missense variants we identify at hotspot positions in *CACNA1B* may be function altering. *KCNG1* has been implicated in neuronal development,[41] and the expression profile matches well with that of the other NDD genes that have hotspot mutations. There is also some circumstantial evidence for two of the other three genes. Both *TPCN1* and *TPCN2* (MIM: 612163) have no prior NDD association, but both genes are part of the mTOR complex, which has previously been associated with NDDs.[39] Phenotypic data for the individual with the missense DNM in *TPCN1* shows that this person has macrocephaly and severe ASD (Data S6), which is in line with the fact that mTOR genes have been associated with intracranial volume and intellectual disability.[53] However, the only *TPCN1* missense mutation presently described in literature at a hotspot position (p.102) is associated with early-onset cardiomyopathy.[54]

In this analysis, we initially identified stringent mutation hotspots statistically using unique missense mutation counts. While MDHS analysis on even larger cohorts may identify additional hotspots, we believe our method could be used on smaller datasets by also considering recurrent mutations. Applying this lenient method to our cohort identified 32 significant missense hotspots (Data S2). Even though the inclusion of recurrent mutations allows hotspots to be driven by proliferative advantages of single mutations in the germline or soma, CpG hypermutability, or biases in clinical ascertainment, it also increases power to detect robust hotspot positions (Figure S6). In support of this, we find an enrichment of likely pathogenic missense variants at lenient hotspot positions in clinical databases even if we look only at codons without a mutation in our cohort, showing the merit of this approach. However, additional filtering may be required to remove hotspots driven solely by recurrent missense mutations. Additionally, there is in principle no reason to restrict this method to *de novo* mutations; it could easily be applied to rare inherited variants in large patient cohorts.

Kaplanis et al.[1] estimate that approximately 350,000 parent-offspring trios would be required to detect the majority of remaining haploinsufficient genes associated with NDDs. Genes enriched for function-altering mutations are predicted to be even more difficult to detect, even in very large cohorts. Methods based on homology, like MDHS, are an approach to the identification of disease genes and mechanisms in existing datasets without increasing cohort size. Additionally, the systematic identification of function-altering mutations in large population datasets will have fundamental impact on our understanding of disease biology and may lead to improvements in patient care. In NDD-associated haploinsufficient genes, we observe that function-altering mutations can have substantially different phenotypes and severities than mutations resulting in loss of function. In the future, affected individuals could be stratified for targeted therapies or counseled about their

prognosis based on the mutational mechanism of their disease-causing variant. More broadly, function-altering mutations will provide insight into the molecular function of protein domains. The way haploinsufficiency causes disease is not domain specific, whereas the function-altering mutations we identify are a specific property of the domain in which they occur. New approaches are required to understand the role of function-altering mutations in the human germline, and we provide compelling evidence that the aggregation of mutations over homologous protein domains could be one of these approaches.

Data and code availability

The published article includes all data generated during this study in Data S1, S2, S3, S4, S5, S6, S7, S8, S9, S10, S11, S12, S13, S14, S15, S16, and S17.

The code and docker configurations generated during this study are available at GitHub (https://github.com/cmbi/MetaDomainHotSpot). Data to reproduce figures and all parts of the analyses in this study are included in this repository.

A local version of MetaDome (https://stuart.radboudumc.nl/metadome/) was used to annotate genomic data with meta-domain information and MetaDome tolerance scores. The original MetaDome source code is available on Github (https://github.com/cmbi/metadome) and all data underlying the MetaDome web server is available on Zenodo (https://zenodo.org/record/6625251).

External *de novo* mutation (DNM) dataset used in this this study are publicly available in the original publications: developmental disorder (NDD) DNMs, Kaplanis et al.[1]; autism spectrum disorder (ASD) DNMs, Satterstrom et al.[2]; congenital heart defect (CHD) DNMs, Jin et al.[3]; DNMs from unaffected individuals, Jonsson et al.,[4] Satterstrom et al.[2]

Expression data used for this work is publicly available through GTEx (https://gtexportal.org/home/), and we have made use GTEx release v.8 for this study.

Supplemental information

Supplemental information can be found online at https://doi.org/10.1016/j.ajhg.2022.12.001.

Acknowledgments

We thank Dr. Torti and Dr. Retterer from GeneDX for connecting us with Prof. Mefford. We thank Prof. Mefford for information regarding the likely NDD-association of *KCHN5*. We thank Elke de Boer for useful discussions. This work was in part financially supported by grants from the Dutch Research Council (NWO) (916-14-043 to C.G. and 918-15-667 to J.A.V.) and from the Radboud Institute for Molecular Life Sciences, Radboud University Medical Center (R0002793 to G.V.).

Declaration of interests

The authors have no competing interests.

Received: July 11, 2022
Accepted: December 2, 2022
Published: December 22, 2022

Web resources

CATH-Gene3D, http://www.cathdb.info/
ClinVar, https://www.ncbi.nlm.nih.gov/clinvar/
DECIPHER, https://www.deciphergenomics.org/
GTEx, https://www.gtexportal.org/home/
HGMD, http://www.hgmd.cf.ac.uk/ac/index.php
MetaDomainHotspot analyses repository, https://github.com/cmbi/MetaDomainHotSpot
MetaDome GitHub repository, https://github.com/cmbi/metadome
MetaDome web server, https://stuart.radboudumc.nl/metadome/
Swiss-Prot, https://www.uniprot.org/
Variant Effect Predictor, https://www.ensembl.org/Tools/VEP
VKGL, https://www.vkgl.nl/nl/diagnostiek/vkgl-datashare-database
YASARA, http://www.yasara.org/

References

1. Kaplanis, J., Samocha, K.E., Wiel, L., Zhang, Z., Arvai, K.J., Eberhardt, R.Y., Gallone, G., Lelieveld, S.H., Martin, H.C., McRae, J.F., et al. (2020). Evidence for 28 genetic disorders discovered by combining healthcare and research data. Nature *586*, 757–762. https://doi.org/10.1038/s41586-020-2832-5.
2. Satterstrom, F.K., Kosmicki, J.A., Wang, J., Breen, M.S., De Rubeis, S., An, J.Y., Peng, M., Collins, R., Grove, J., Klei, L., et al. (2020). Large-Scale Exome Sequencing Study Implicates Both Developmental and Functional Changes in the Neurobiology of Autism. Cell *180*, 568–584. e23.
3. Jin, S.C., Homsy, J., Zaidi, V., Lu, Q., Morton, S., DePalma, S.R., Zeng, X., Qi, H., Chang, W., Sierant, M.C., et al. (2017). Contribution of rare inherited and de novo variants in 2,871 congenital heart disease probands. Nat Genet *49*, 1593–1601.
4. Jónsson, H., Sulem, P., Kehr, B., Kristmundsdottir, S., Zink, F., Hjartarson, E., Hardarson, M.T., Hjorleifsson, K.E., Eggertsson, H.P., Gudjonsson, S.A., et al. (2017). Parental influence on human germline de novo mutations in 1,548 trios from Iceland. Nature *549*, 519–522.
5. Veltman, J. a, and Brunner, H.G. (2012). De novo mutations in human genetic disease. Nat. Rev. Genet. *13*, 565–575.
6. Martin, H.C., Jones, W.D., McIntyre, R., Sanchez-Andrade, G., Sanderson, M., Stephenson, J.D., Jones, C.P., Handsaker, J., Gallone, G., Bruntraeger, M., et al. (2018). Quantifying the contribution of recessive coding variation to developmental disorders. Science *362*, 1161–1164.
7. Deciphering Developmental Disorders Study (2017). Prevalence and architecture of de novo mutations in developmental disorders. Nature *542*, 433–438.
8. de Ligt, J., Willemsen, M.H., van Bon, B.W.M., Kleefstra, T., Yntema, H.G., Kroes, T., Vulto-van Silfhout, A.T., Koolen, D.A., de Vries, P., Gilissen, C., et al. (2012). Diagnostic exome sequencing in persons with severe intellectual disability. N. Engl. J. Med. *367*, 1921–1929.
9. Deciphering Developmental Disorders Study (2015). Large-scale discovery of novel genetic causes of developmental disorders. Nature *519*, 223–228.
10. Turner, T.N., Yi, Q., Krumm, N., Huddleston, J., Hoekzema, K., F Stessman, H.A., Doebley, A.L., Bernier, R.A., Nickerson, D.A., and Eichler, E.E. (2017). a compendium of human de novo variants. Nucleic Acids Res. *45*, D804–D811.
11. Geisheker, M.R., Heymann, G., Wang, T., Coe, B.P., Turner, T.N., Stessman, H.A.F., Hoekzema, K., Kvarnung, M., Shaw, M., Friend, K., et al. (2017). Hotspots of missense mutation

identify neurodevelopmental disorder genes and functional domains. Nat. Neurosci. *20*, 1043–1051.
12. Lelieveld, S.H., Wiel, L., Venselaar, H., Pfundt, R., Vriend, G., Veltman, J.A., Brunner, H.G., Vissers, L.E.L.M., and Gilissen, C. (2017). Spatial clustering of de novo missense mutations identifies candidate neurodevelopmental disorder-associated genes. Am. J. Hum. Genet. *101*, 478–484.
13. Wiel, L., Venselaar, H., Veltman, J.A., Vriend, G., and Gilissen, C. (2017). Aggregation of population-based genetic variation over protein domain homologues and its potential use in genetic diagnostics. Hum. Mutat. *38*, 1454–1463. https://doi.org/10.1002/humu.23313.
14. Stenson, P.D., Mort, M., Ball, E.V., Evans, K., Hayden, M., Heywood, S., Hussain, M., Phillips, A.D., and Cooper, D.N. (2017). The Human Gene Mutation Database: towards a comprehensive repository of inherited mutation data for medical research, genetic diagnosis and next-generation sequencing studies. Hum. Genet. *136*, 665–677.
15. Landrum, M.J., Lee, J.M., Benson, M., Brown, G., Chao, C., Chitipiralla, S., Gu, B., Hart, J., Hoffman, D., Hoover, J., et al. (2016). ClinVar: public archive of interpretations of clinically relevant variants. Nucleic Acids Res. *44*, D862–D868.
16. Schuurs-Hoeijmakers, J.H.M., Oh, E.C., Vissers, L.E.L.M., Swinkels, M.E.M., Gilissen, C., Willemsen, M.A., Holvoet, M., Steehouwer, M., Veltman, J.A., de Vries, B.B.A., et al. (2012). Recurrent de novo mutations in PACS1 cause defective cranial-neural-crest migration and define a recognizable intellectual-disability syndrome. Am. J. Hum. Genet. *91*, 1122–1127.
17. Wiel, L., Baakman, C., Gilissen, D., Veltman, J.A., Vriend, G., and Gilissen, C. (2019). MetaDome: pathogenicity analysis of genetic variants through aggregation of homologous human protein domains. Hum. Mutat. *40*, 1030–1038.
18. Peterson, T.A., Park, D., and Kann, M.G. (2013). A protein domain-centric approach for the comparative analysis of human and yeast phenotypically relevant mutations. BMC Genom. *14*, S5.
19. Yue, P., Forrest, W.F., Kaminker, J.S., Lohr, S., Zhang, Z., and Cavet, G. (2010). Inferring the functional effects of mutation through clusters of mutations in homologous proteins. Hum. Mutat. *31*, 264–271.
20. Peterson, T.A., Nehrt, N.L., Park, D., and Kann, M.G. (2012). Incorporating molecular and functional context into the analysis and prioritization of human variants associated with cancer. J. Am. Med. Inform. Assoc. *19*, 275–283.
21. Retterer, K., Juusola, J., Cho, M.T., Vitazka, P., Millan, F., Gibellini, F., Vertino-Bell, A., Smaoui, N., Neidich, J., Monaghan, K.G., et al. (2016). Clinical application of whole-exome sequencing across clinical indications. Genet. Med. *18*, 696–704.
22. Wright, C.F., Fitzgerald, T.W., Jones, W.D., Clayton, S., McRae, J.F., van Kogelenberg, M., King, D.A., Ambridge, K., Barrett, D.M., Bayzetinova, T., et al. (2015). Genetic diagnosis of developmental disorders in the DDD study: a scalable analysis of genome-wide research data. Lancet *385*, 1305–1314.
23. Lelieveld, S.H., Reijnders, M.R.F., Pfundt, R., Yntema, H.G., Kamsteeg, E.J., de Vries, P., de Vries, B.B.A., Willemsen, M.H., Kleefstra, T., Löhner, K., et al. (2016). Meta-analysis of 2, 104 trios provides support for 10 new genes for intellectual disability. Nat. Neurosci. *19*, 1194–1196.
24. Harrow, J., Frankish, A., Gonzalez, J.M., Tapanari, E., Diekhans, M., Kokocinski, F., Aken, B.L., Barrell, D., Zadissa, A., Searle, S., et al. (2012). GENCODE: The reference human genome annotation for The ENCODE Project. Genome Res. *22*, 1760–1774.
25. Boutet, E., Lieberherr, D., Tognolli, M., Schneider, M., Bansal, P., Bridge, A.J., Poux, S., Bougueleret, L., and Xenarios, I. (2016). UniProtKB/Swiss-Prot, the manually annotated section of the UniProt KnowledgeBase: how to use the entry view. Methods Mol. Biol. *1374*, 23–54.
26. Finn, R.D., Coggill, P., Eberhardt, R.Y., Eddy, S.R., Mistry, J., Mitchell, A.L., Potter, S.C., Punta, M., Qureshi, M., Sangrador-Vegas, A., et al. (2016). The Pfam protein families database: towards a more sustainable future. Nucleic Acids Res. *44*, D279–D285.
27. McLaren, W., Gil, L., Hunt, S.E., Riat, H.S., Ritchie, G.R.S., Thormann, A., Flicek, P., and Cunningham, F. (2016). The Ensembl Variant Effect Predictor. Genome Biol. *17*, 122–214.
28. Karczewski, K.J., Francioli, L.C., Tiao, G., Cummings, B.B., Alföldi, J., Wang, Q., Collins, R.L., Laricchia, K.M., Ganna, A., Birnbaum, D.P., et al. (2020). The mutational constraint spectrum quantified from variation in 141, 456 humans. Nature *581*, 434–443.
29. Kumar, P., Henikoff, S., and Ng, P.C. (2009). Predicting the effects of coding non-synonymous variants on protein function using the SIFT algorithm. Nat. Protoc. *4*, 1073–1081.
30. Adzhubei, I.A., Schmidt, S., Peshkin, L., Ramensky, V.E., Gerasimova, A., Bork, P., Kondrashov, A.S., and Sunyaev, S.R. (2010). A method and server for predicting damaging missense mutations. Nat. Methods *7*, 248–249.
31. Samocha, K.E., Kosmicki, J.A., Karczewski, K.J., O'Donnell-Luria, A.H., Pierce-Hoffman, E., MacArthur, D.G., Neale, B.M., and Daly, M.J. (2017). Regional missense constraint improves variant deleteriousness prediction. Preprint at bioRxiv. https://doi.org/10.1101/148353.
32. Kircher, M., Witten, D.M., Jain, P., O'Roak, B.J., Cooper, G.M., and Shendure, J. (2014). A general framework for estimating the relative pathogenicity of human genetic variants. Nat. Genet. *46*, 310–315.
33. Richards, S., Aziz, N., Bale, S., Bick, D., Das, S., Gastier-Foster, J., Grody, W.W., Hegde, M., Lyon, E., Spector, E., et al. (2015). Standards and guidelines for the interpretation of sequence variants: a joint consensus recommendation of the American College of Medical Genetics and Genomics and the Association for Molecular Pathology. Genet. Med. *17*, 405–424.
34. Krieger, E., Koraimann, G., and Vriend, G. (2002). Increasing the precision of comparative models with YASARA NOVA—a self-parameterizing force field. Proteins *47*, 393–402.
35. Vriend, G. (1990). WHAT IF: A molecular modeling and drug design program. J. Mol. Graph. *8*, 52–56.
36. Lek, M., Karczewski, K.J., Minikel, E.V., Samocha, K.E., Banks, E., Fennell, T., O'Donnell-Luria, A.H., Ware, J.S., Hill, A.J., Cummings, B.B., et al. (2016). Analysis of protein-coding genetic variation in 60, 706 humans. Nature *536*, 285–291.
37. Aguet, F., et al. (2020). The GTEx Consortium atlas of genetic regulatory effects across human tissues. Science *369*, 1318–1330.
38. GTEx Consortium, Battle, A., Brown, C.D., Engelhardt, B.E., and Montgomery, S.B. (2017). Genetic effects on gene expression across human tissues. Nature *550*, 204–213.
39. Cang, C., Zhou, Y., Navarro, B., Seo, Y.J., Aranda, K., Shi, L., Battaglia-Hsu, S., Nissim, I., Clapham, D.E., and Ren, D.

(2013). mTOR regulates lysosomal ATP-sensitive two-pore Na(+) channels to adapt to metabolic state. Cell *152*, 778–790.
40. Veeramah, K.R., Johnstone, L., Karafet, T.M., Wolf, D., Sprissler, R., Salogiannis, J., Barth-Maron, A., Greenberg, M.E., Stuhlmann, T., Weinert, S., et al. (2013). Exome sequencing reveals new causal mutations in children with epileptic encephalopathies. Epilepsia *54*, 1270–1281.
41. Chiocchetti, A.G., Haslinger, D., Stein, J.L., de la Torre-Ubieta, L., Cocchi, E., Rothämel, T., Lindlar, S., Waltes, R., Fulda, S., Geschwind, D.H., and Freitag, C.M. (2016). Transcriptomic signatures of neuronal differentiation and their association with risk genes for autism spectrum and related neuropsychiatric disorders. Transl. Psychiatry *6*. e864–e864.
42. Gorman, K.M., Meyer, E., Grozeva, D., Spinelli, E., McTague, A., Sanchis-Juan, A., Carss, K.J., Bryant, E., Reich, A., Schneider, A.L., et al. (2019). Bi-allelic Loss-of-Function CACNA1B Mutations in Progressive Epilepsy-Dyskinesia. Am. J. Hum. Genet. *104*, 948–956.
43. Sillitoe, I., Lewis, T., and Orengo, C. (2015). Using CATHGene3D to analyze the sequence, structure, and function of proteins. Curr. Protoc. Bioinformatics *50*, 1.28.1–1.28.21.
44. Bezanilla, F. (2008). How membrane proteins sense voltage. Nat. Rev. Mol. Cell Biol. *9*, 323–332.
45. Sands, T.T., Miceli, F., Lesca, G., Beck, A.E., Sadleir, L.G., Arrington, D.K., Schönewolf-Greulich, B., Moutton, S., Lauritano, A., Nappi, P., et al. (2019). Autism and developmental disability caused by KCNQ3 gain-of-function variants. Ann. Neurol. *86*, 181–192.
46. Luo, X., Rosenfeld, J.A., Yamamoto, S., Harel, T., Zuo, Z., Hall, M., Wierenga, K.J., Pastore, M.T., Bartholomew, D., Delgado, M.R., et al. (2017). Clinically severe CACNA1A alleles affect synaptic function and neurodegeneration differentially. PLoS Genet. *13*, e1006905.
47. Kortüm, F., Caputo, V., Bauer, C.K., Stella, L., Ciolfi, A., Alawi, M., Bocchinfuso, G., Flex, E., Paolacci, S., Dentici, M.L., et al. (2015). Mutations in KCNH1 and ATP6V1B2 cause Zimmermann-Laband syndrome. Nat. Genet. *47*, 661–667.
48. Daniil, G., Fernandes-Rosa, F.L., Chemin, J., Blesneac, I., Beltrand, J., Polak, M., Jeunemaitre, X., Boulkroun, S., Amar, L., Strom, T.M., et al. (2016). CACNA1H mutations are associated with different forms of primary aldosteronism. EBioMedicine *13*, 225–236.
49. Zhang, X.Y., Wen, J., Yang, W., Wang, C., Gao, L., Zheng, L.H., Wang, T., Ran, K., Li, Y., Li, X., et al. (2013). Gain-of-function mutations in SCN11A cause familial episodic pain. Am. J. Hum. Genet. *93*, 957–966.
50. Heyne, H.O., Singh, T., Stamberger, H., Abou Jamra, R., Caglayan, H., Craiu, D., De Jonghe, P., Guerrini, R., Helbig, K.L., Koeleman, B.P.C., et al. (2018). De novo variants in neurodevelopmental disorders with epilepsy. Nat. Genet. *50*, 1048–1053.
51. Heyne, H.O., Baez-Nieto, D., Iqbal, S., Palmer, D.S., Brunklaus, A., May, P., Epi25 Collaborative, Johannesen, K.M., Lauxmann, S., Lemke, J.R., et al. (2020). Predicting functional effects of missense variants in voltage-gated sodium and calcium channels. Sci. Transl. Med. *12*, eaay6848.
52. Happ, H.C., Sadleir, L.G., Zemel, M., de Valles-Ibáñez, G., Hildebrand, M.S., McConkie-Rosell, A., et al. (2022). Neurodevelopmental and Epilepsy Phenotypes in Individuals With Missense Variants in the Voltage Sensing and Pore Domain of KCNH5. Neurology. Published online October *28*, 2022. https://doi.org/10.1212/WNL.0000000000201492.
53. Reijnders, M.R.F., Kousi, M., van Woerden, G.M., Klein, M., Bralten, J., Mancini, G.M.S., van Essen, T., Proietti-Onori, M., Smeets, E.E.J., van Gastel, M., et al. (2017). Variation in a range of mTOR-related genes associates with intracranial volume and intellectual disability. Nat. Commun. *8*, 1052.
54. Reuter, M.S., Chaturvedi, R.R., Liston, E., Manshaei, R., Aul, R.B., Bowdin, S., Cohn, I., Curtis, M., Dhir, P., Hayeems, R.Z., et al. (2020). The cardiac genome clinic: implementing genome sequencing in pediatric heart disease. Genet. Med. *22*, 1015–1024.

The American Journal of Human Genetics, Volume *110*

Supplemental information

De novo mutation hotspots in homologous protein domains identify function-altering mutations in neurodevelopmental disorders

Laurens Wiel, Juliet E. Hampstead, Hanka Venselaar, Lisenka E.L.M. Vissers, Han G. Brunner, Rolph Pfundt, Gerrit Vriend, Joris A. Veltman, and Christian Gilissen

Contents

Supplementary Data

Data S1. De novo mutations
Data_S1_Kaplanis_DNMs_metadomain_annotation.csv

Data S2. De novo mutation missense hotspot results
Data_S2_missense_DNM_hotspot_results.xlsx

Data S3. De novo mutation synonymous hotspot results
Data_S3_synonymous_DNM_hotspot_results.xlsx

Data S4. De novo mutation nonsense hotspot results
Data_S4_nonsense_DNM_hotspot_results.xlsx

Data S5. De novo mutations at significant hotspot
Data_S5_variants_at_hotspots_VEP_annotated.xlsx

Data S6. Phenotypes of patients with missense mutations at hotspot positions
Data_S6_Phenotypes_of_patients_with_hotspots.xlsx

Data S7. YASARA structures
Data_S7_YASARA_structures_hotspots.sce

Data S8. Structural effects of missense DNMs at hotspots
Data_S8_hotspot_variants_structural_effects.xlsx

Data S9. Gene sets used in analysis
Data_S9_Gene_sets_all.txt

Data S10. PF00520 domain-containing genes used in analysis
Data_S10_Gene_sets_PF00520.txt

Data S11. Mutational constraint in hotspot and proposed novel hotspot genes
Data_S11_Constraint.txt

Data S12. Proportion of hotspot genes expressed across tissues
Data_S12_Hotspot_tissue_expression.txt

Data S13. Proportion of hotspot genes expressed across tissues, PF00520 domain-containing genes
Data_S13_Hotspot_tissue_expression_PF00520.txt

Data S14 Probability density functions for the classification of proposed novel hotspot genes
Data_S14_PDFs_for_proposed_novel_classification.txt

Data S15. Variants at lenient count hotspots
Data_S15_variants_at_lenient_count_hotspots.xlsx

Data S16. Variation at stringent hotspot positions in clinical databases
Data_S17_Variation_at_hotspot_positions_databases.txt

Data S17. All variants at from patients with variant at a novel hotspot gene
Data_S17_all_other_variants_from_patients.csv

Supplementary Figures

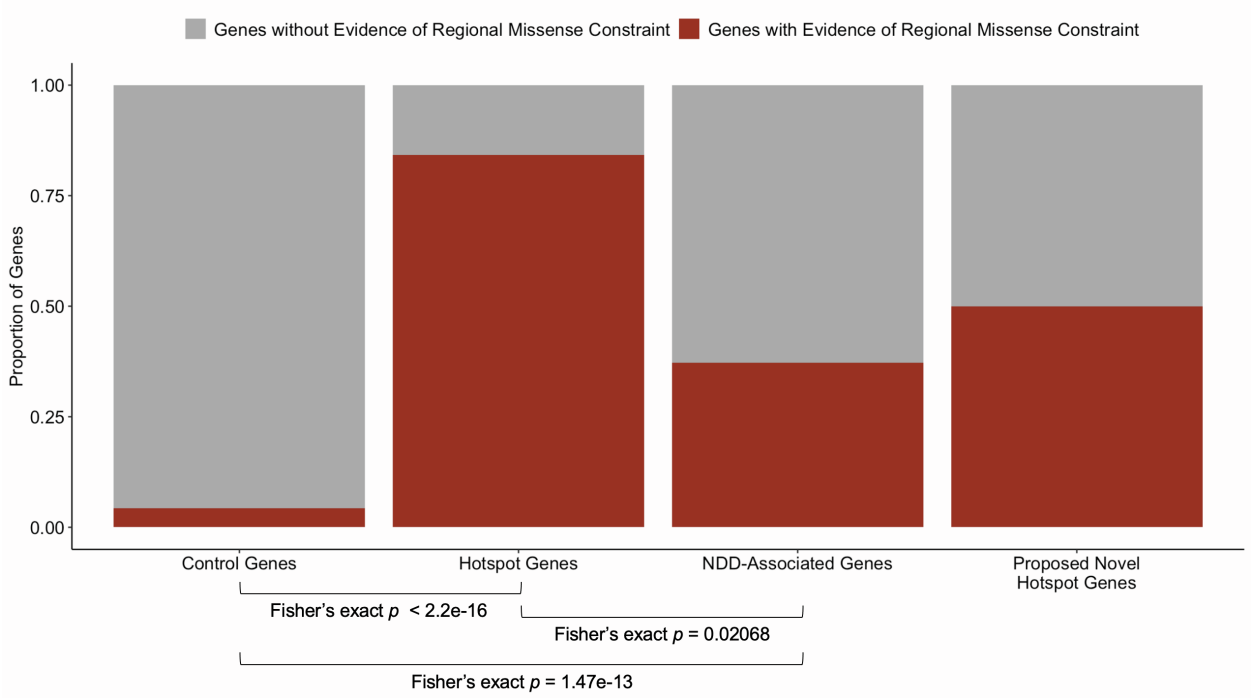

Figure S1. A significant proportion of hotspot genes have evidence of regional missense constraint compared to control and NDD-associated genes.

Genes with evidence of regional missense constraint were taken from Samocha *et al.* (see **Methods**).[1] The proportion of genes with and without evidence of regional missense constraint in this list were compared for control genes, NDD-associated genes, hotspot genes, and proposed novel hotspot genes. Hotspot genes have a significantly higher proportion of genes with regional missense constraint compared to control genes (Fisher's exact $p < 2.2 \times 10^{-16}$) and other NDD-associated genes (Fisher's exact $p = 0.02$).

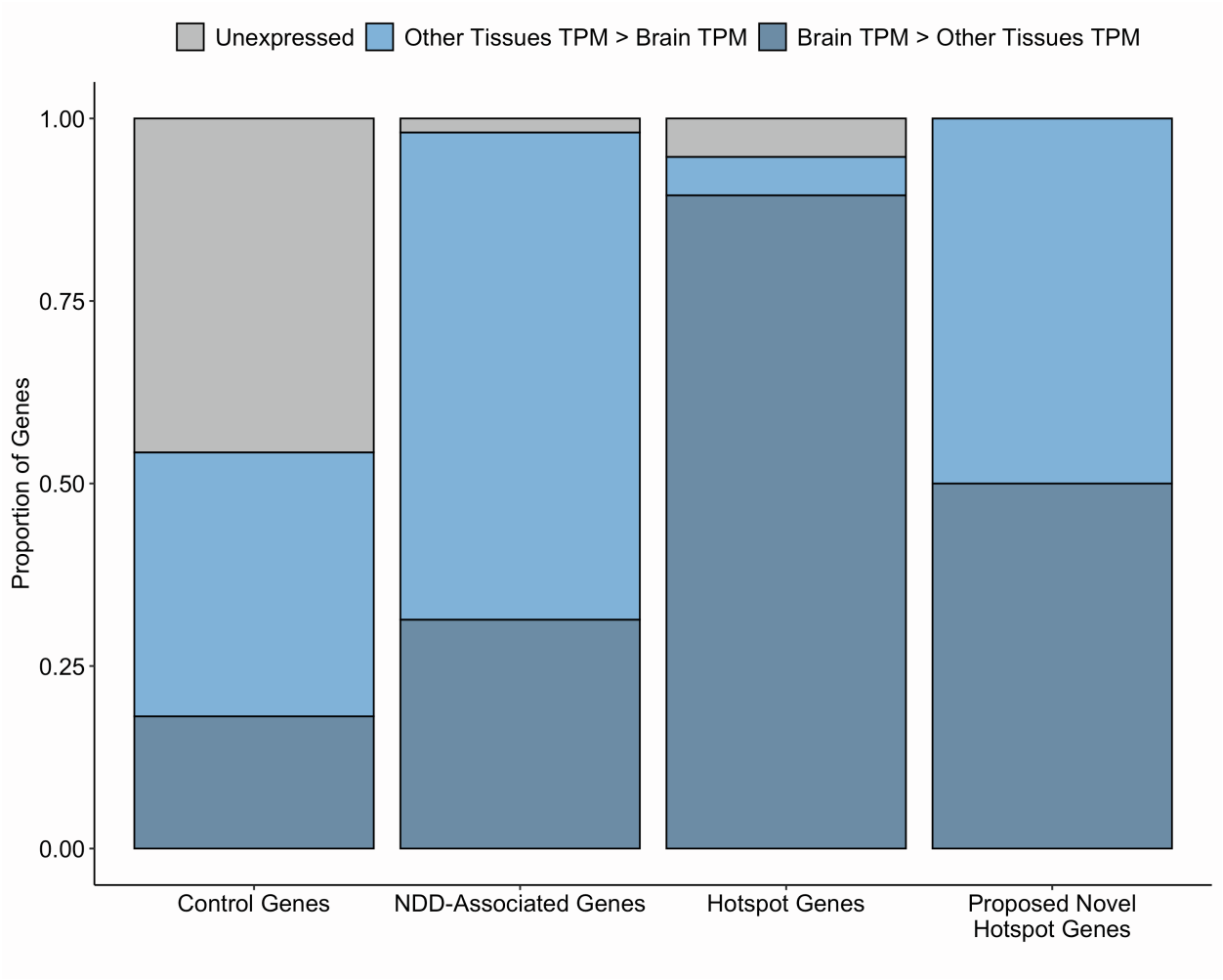

Figure S2. A higher proportion of hotspot genes are expressed in brain than NDD-associated or control genes.

We compared the proportion of unexpressed genes (grey), genes expressed higher in other tissues than in brain by median TPM (light blue), and genes expressed higher in brain than in other tissues by median TPM (dark blue) across four gene sets (control genes, NDD-associated genes, hotspot genes, and proposed novel hotspot genes, see **Methods**). A significantly greater proportion of hotspot genes are expressed in brain than control genes (Fisher's exact $p = 2.985 \times 10^{-5}$) and NDD-associated genes (Fisher's exact $p = 0.002$).

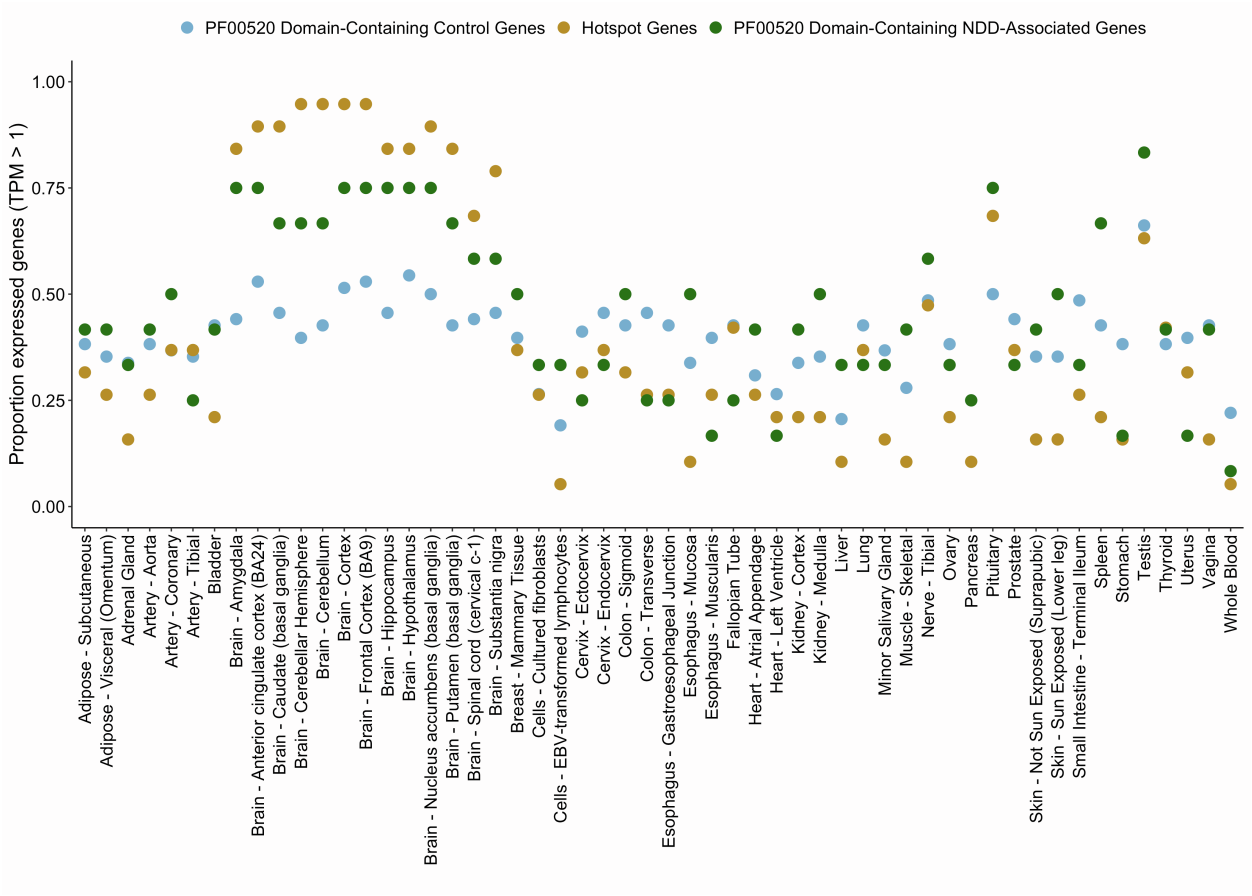

Figure S3. Proportion of hotspot genes expressed across tissues compared to PF00520 domain-containing NDD-associated genes and PF00520 domain-containing control genes.

To determine whether the unique expression profile we observed for our hotspot genes was characteristic of all PF00520 domain-containing genes, we compared hotspot genes to NDD-associated genes containing a PF0050 domain (green, n = 12) and control genes containing a PF00520 domain (blue, n = 68) without sampling. A significantly greater proportion of hotspot genes are expressed in the caudate (basal ganglia), cerebellar hemisphere, cerebellum, cortex, and frontal cortex (BA9) compared to control genes (see **Supplementary Data S11** for Bonferroni-corrected Fisher's exact p-values across all tissues). We find no significant differences between NDD-associated genes containing a PF00520 domain and hotspot genes (**Supplementary Data S11**). We conclude that most NDD-associated PF00520 domain containing genes (n = 31) are expressed in brain, and we have statistical power to detect mutation hotspots in 19 of these genes.

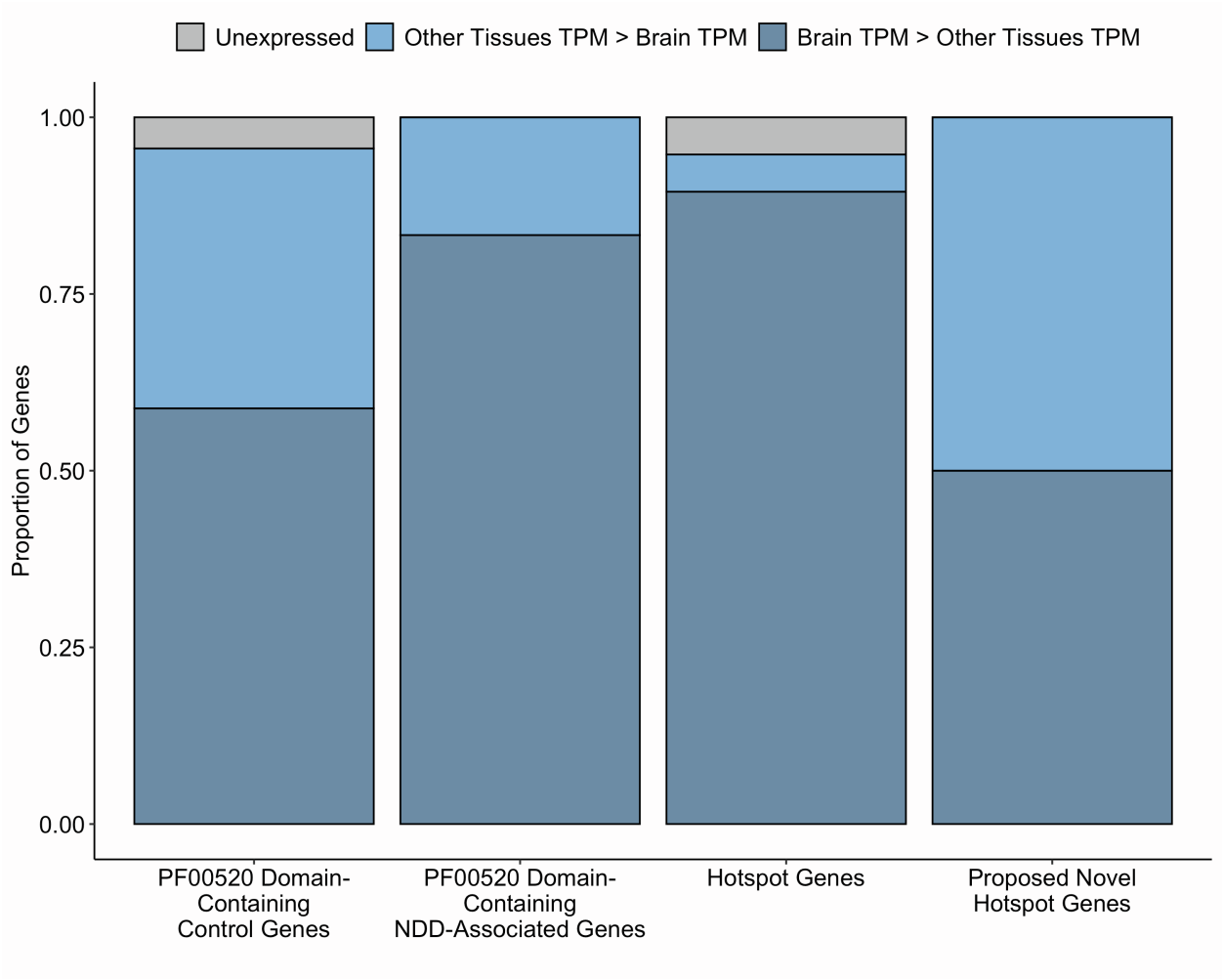

Figure S4. A higher proportion of hotspot genes are expressed in brain than PF00520 domain-containing control genes.

In addition to looking at the proportion of genes expressed in a given tissue, we also considered whether hotspot genes were enriched for higher expression in brain than in other tissues. We show that a significant proportion of hotspot genes have higher expression in brain than in other tissues compared to control genes containing a PF00520 domain (Fisher's exact $p = 0.008$), but not NDD-associated genes also containing this domain (Fisher's exact $p = 0.54$). Hotspot genes likely represent a subset of NDD-associated PF00520 domain-containing genes, and all genes of this class could harbour pathogenic variation at hotspot positions.

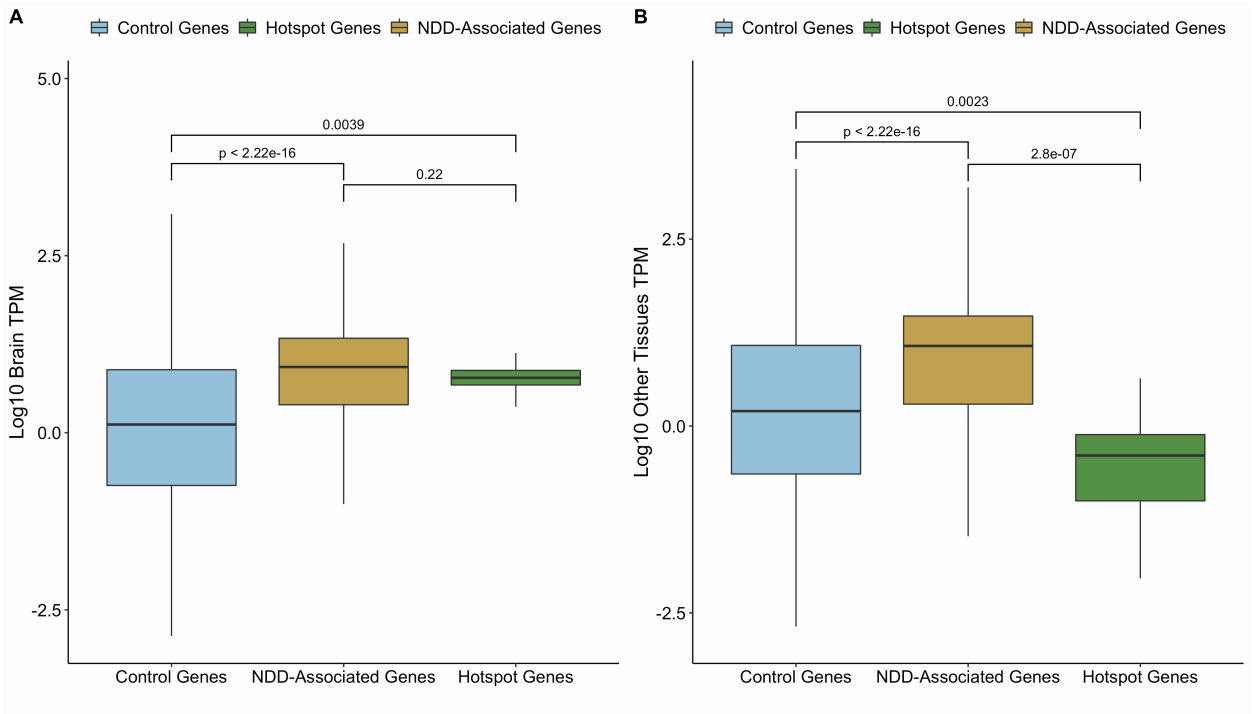

Figure S5. TPM differences between hotspot, NDD-associated, and control genes in brain and other tissues.

We compared the median TPM distribution in brain (A) and other tissues (B) in expressed (TPM > 1) control, NDD-associated, and hotspot genes. We show that both NDD-associated and hotspot genes have higher expression in brain than control genes (Wilcoxon $p < 2.2 \times 10^{-16}$; Wilcoxon $p = 0.0039$). We also show that hotspot genes have significantly lower expression in other tissues compared to both control genes (Wilcoxon $p = 0.0023$) and NDD-associated genes (Wilcoxon $p < 2.2 \times 10^{-16}$). We use these expression differences to associate proposed novel hotspot genes with NDDs (see **Methods**).

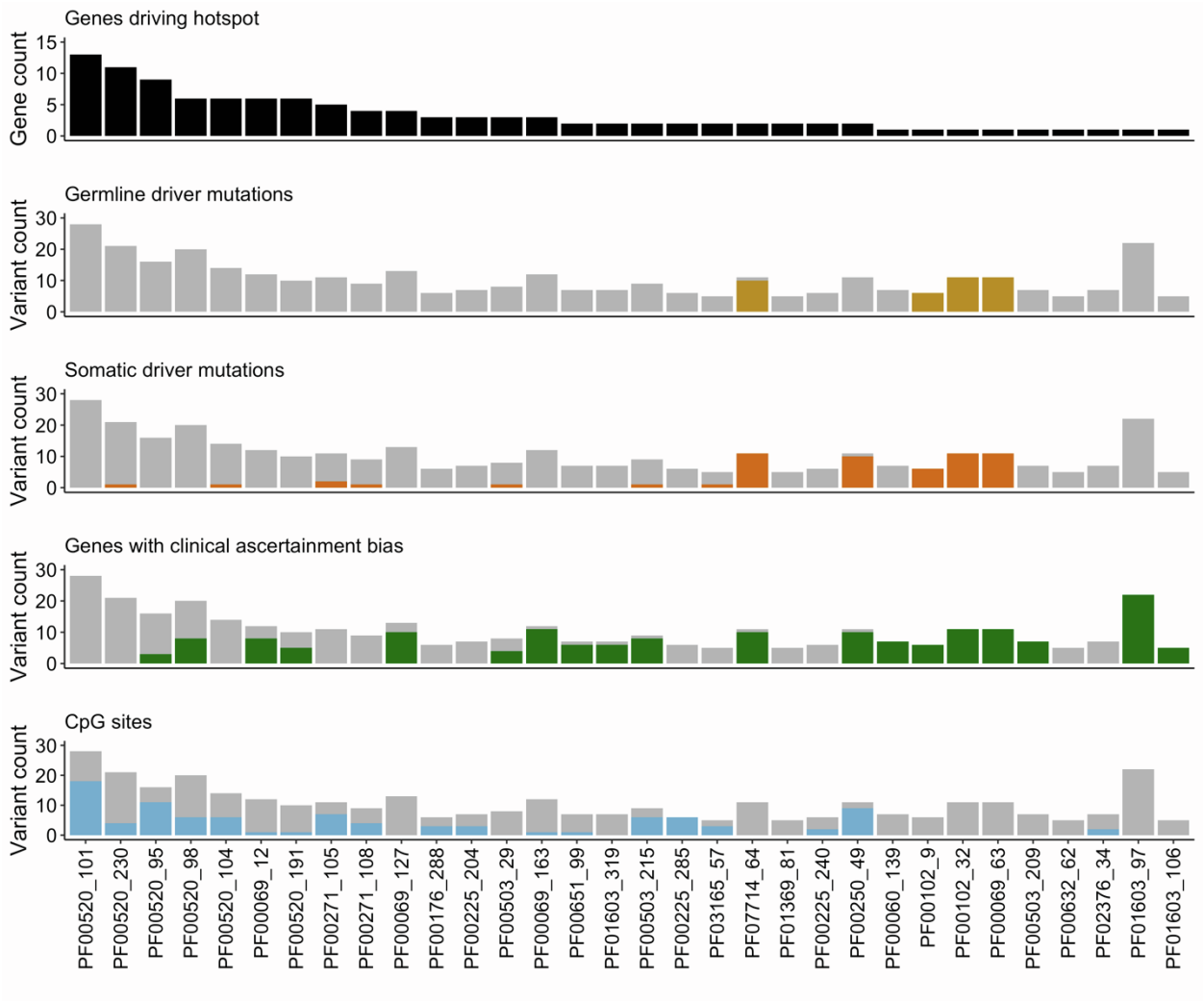

Figure S6. Lenient hotspots may be driven by germline or somatic driver mutations, clinical ascertainment bias, and CpG hypermutability

Lenient hotspots may be driven by variants at the same protein consensus position but different genetic positions, the same genetic position recurrently mutated, or both. Kaplanis *et al.* describe recurrent missense variants as those mutated > 9 times in our cohort, and show that these are driven by four major processes: mutations that confer a proliferative advantage in the germline (germline drivers), mutations that confer a proliferative advantage in somatic tissues (somatic drivers), biases in clinical ascertainment and CpG hypermutability. We considered which of these factors might be driving our lenient mutation hotspots (sorted by the number of genes with mutations at the hotspot, black, top panel) by considering the proportion of mutations at each position driven by these four factors. Mutations in genes known to confer a proliferative advantage in the germline (second panel, yellow) and in the somatic tissue (third panel, orange) are coloured as a proportion of the total number of missense variants at the hotspot. Similarly, genes with clinical ascertainment bias – described here as those in the top 5% of the recurrent missense variant distribution – are coloured in green (fourth panel), and mutations at CpG sites are coloured blue (fifth panel).

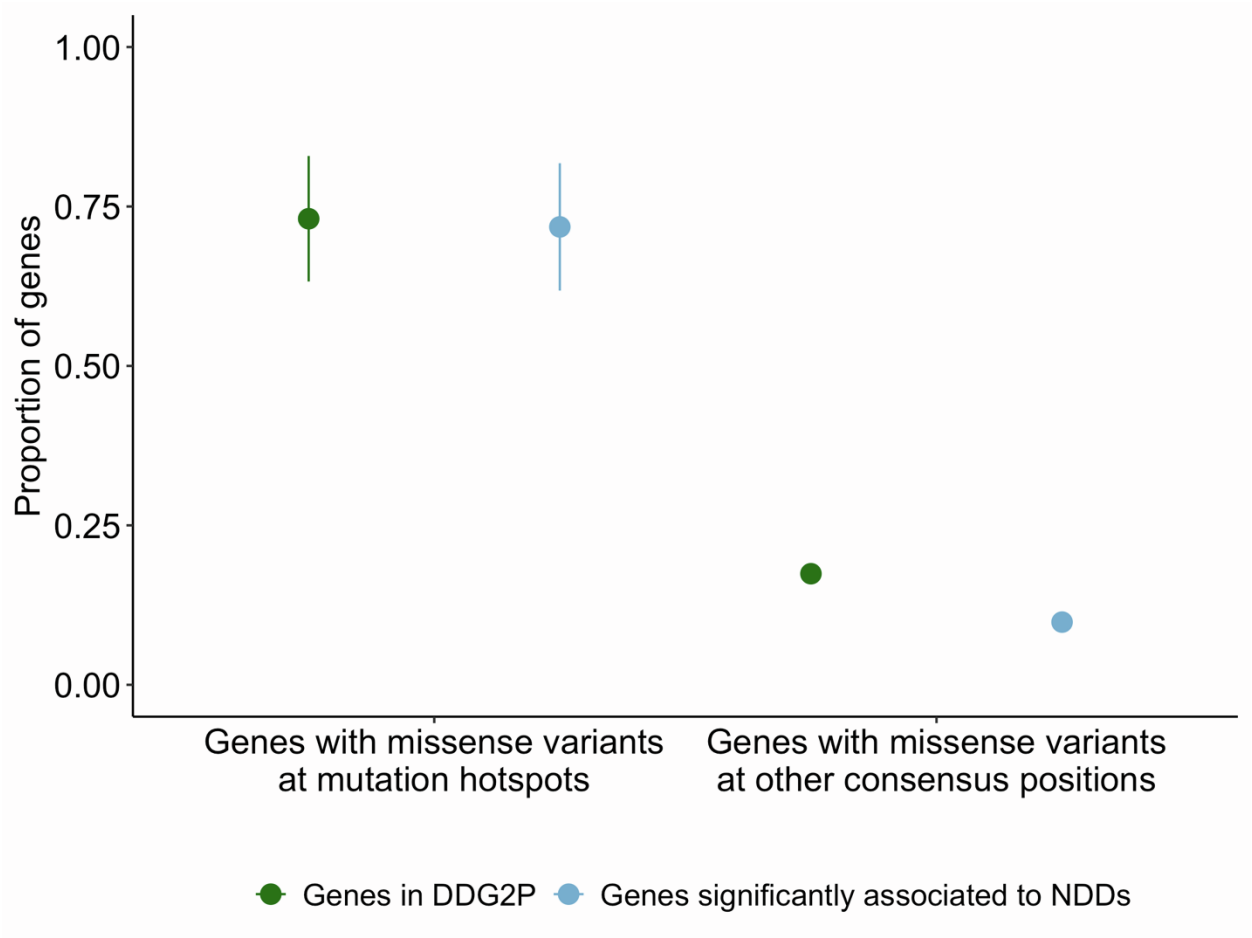

Figure S7. Lenient hotspots are enriched for NDD-associated and DDG2P genes

The proportion of lenient hotspot missense variants in genes statistically associated to NDDs (blue) and in DDG2P (green) is shown at mutation hotspots (left) and all other protein consensus positions (right). Mutation hotspots are significantly enriched for missense mutations in genes statistically associated to NDDs (Fisher's exact $p < 2.2 \times 10^{-16}$) and in DDG2P (Fisher's exact $p < 2.2 \times 10^{-16}$).

Supplementary Tables

	SNV PTVs	Missense variants	Synonymous variants	Total variants
ASD (Satterstrom *et al.*)	128	1883	714	2725
CHD (Jin *et al.*)	45	741	235	1021
Unaffected (Jonsson *et al.*, Satterstrom *et al.*)	60	1377	524	1961

Table S1 – Counts of PTV, missense, and synonymous variants in protein domains in external de novo mutation datasets

All DNMs from Satterstrom et al. (autism-spectrum disorders, ASD), Jin et al. (congenital heart defects, CHD) and unaffected individuals (Jonsson et al., Satterstrom et al. unaffected siblings) were mapped to metadomains for our hotspot analysis. The number of SNV PTVs (stop_gained), missense variants, and synonymous variants in protein domains are shown per cohort.

	Original	MetaDomain Annotated	Located in Pfam Protein Domain	Meta-Domain Position Annotated
Missense	28,241	26,178	13,114	11,288
Synonymous	9,005	8,496	3,862	3,229
Stop-gained	2,685	2,415	926	805
Total	39,931	37,089	17,902	15,322

Table S2 – NDD DNMs after processing

*Description of DNMs from Kaplanis et. al. study[4] after DNM annotation and filtering (see **Methods**).*

Hotspot Position	Total Missense Variants at Position	Unique Missense Variants at Position
p.96	16	10
p.102	20	13
p.231	21	14

Table S3 – Missense variant counts at hotspot positions p.96, p.102, p.231

The number of missense variants at each hotspot position is summarised. The total missense variants represent all variants at the protein consensus position, including identical variants. Unique variants are counted as all unique chromosome, position, ref, alt at a protein consensus position without the inclusion of identical variants.

	With Missense DNMs at Significant Hotspot	Without Missense DNMs at Significant Hotspot	Total
DD-associated Genes	19	596	615
Other Genes	6	4,998	5,004
Total	25	5,594	5,619

Table S4 – Genes with missense DNMs hotspots by unique counting

A comparison of NDD-associated genes and genes not associated to NDD from the perspective of significant missense DNM identified via unique counting of DNMs. Contingency table (Chi-square $p = 1.11^{-13}$, test-statistic = 55.17, degrees of freedom = 1) featuring counts of genes that have missense DNMs in a potential hotspot location: i.e. located at a position that can be aggregated via homologous protein domain relations. Both the missense DNMs and diagnostic lists result from the Kaplanis et al. study.[4] Based on this data, NDD-associated genes are by a 3.17 fold more likely to have a significant missense DNM hotspot than genes that do not have NDD-association.

	Function-Altering Mutation Consequence	Other Mutation Consequence
Hotspot genes in DDG2P	6	10
Other DDG2P Genes	163	1967

Table S5 – Hotspot genes are enriched for gain-of-function mutation consequences in DDG2P
*Hotspot genes were tested for an enrichment of function-altering mutation consequences (see **Methods**). Genes can belong to only one class (hotspot or other DDG2P genes), but their mutation consequences are considered independent (they can have both a function-altering mutation consequence and a different mutation consequence provided they are both in DDG2P). Function-altering mutation consequences were enriched in the hotspot gene set in DDG2P compared to other genes (Fisher's exact p-value = 5.484×10^{-5}).*

	Constitutively Expressed	Not Constitutively Expressed	Unexpressed	Total Not Constitutively Expressed
Control Genes	7853	23052	24278	47330
NDD-Associated Genes	476	505	11	516

Table S6 – NDD-associated genes have higher levels of constitutive expression than control genes
To show that NDD-associated genes generally have higher constitutive expression than control genes, we counted constitutively expressed (TPM > 1 in all tissues) and not constitutively expressed (TPM <= 1 in all tissues) genes in each set in GTEx data. NDD-associated genes have significantly higher levels of constitutive expression than control genes, even if we just consider genes in both sets that are expressed (TPM > 1 in at least one tissue; Fisher's exact $p < 2.2 \times 10^{-16}$ in both sets).

	With missense DNMs at significant hotspot	Without missense DNMs at significant hotspot	Total
NDD-Associated Genes	48	567	615
Other Genes	19	4,985	5,004
Total	67	5,552	5,619

Table S7 – Genes with lenient missense hotspots

A comparison of NDD-associated genes and genes not associated to NDD from the perspective of significant missense DNM hotspots identified via lenient counting of DNMs. Contingency table (Chi-square $p = 1.26^{-31}$, test-statistic = 136.92, degrees of freedom = 1) featuring counts of genes that have missense DNMs in a potential hotspot location: i.e. located at a position that can be aggregated via homologous protein domain relations. Both the missense DNMs and diagnostic lists result from the Kaplanis et al. study.[4] Based on this data, NDD-associated genes are by a 2.53 fold more likely to have a significant missense DNM hotspot than genes that do not have NDD-association.

VKGL:

	Hotspot consensus positions	Other consensus positions
Likely pathogenic variants	61	3314
Likely benign variants	3	9465

Fisher's exact $p < 2.2 \times 10^{-16}$

	Hotspot consensus positions (no DNM at position)	Other consensus positions (no DNM at position)
Likely pathogenic variants	32	3154
Likely benign variants	3	9429

Fisher's exact $p < 2.2 \times 10^{-16}$

	Hotspot consensus positions (no DNM at codon)	Hotspot consensus positions (no DNM at codon)
Likely pathogenic variants	26	3096
Likely benign variants	3	9398

Fisher's exact $p = 3.08 \times 10^{-13}$

ClinVar:

	Hotspot consensus positions	Other consensus positions
Likely pathogenic variants	176	12985
Likely benign variants	9	12335

Fisher's exact $p < 2.2 \times 10^{-16}$

	Hotspot consensus positions (no DNM at position)	Other consensus positions (no DNM at position)
Likely pathogenic variants	121	12074
Likely benign variants	9	12294

Fisher's exact $p < 2.2 \times 10^{-16}$

	Hotspot consensus positions (no DNM at codon)	Hotspot consensus positions (no DNM at codon)
Likely pathogenic variants	104	11861
Likely benign variants	9	12254

Fisher's exact $p < 2.2 \times 10^{-16}$

Table S8 – Lenient hotspot positions are enriched for likely pathogenic missense variation in clinical databases

We compared the proportion of likely pathogenic missense variants at hotspot positions versus all other protein consensus positions in VKGL (top) and ClinVar (bottom). We compared all positions (first table), positions without a DNM at our cohort (second table), and positions without a DNM in the codon in our cohort (third table). Statistical significance was calculated using Fisher's exact test.

	Hotspot consensus position missense DNMs	Other consensus position missense DNMs
NDD probands	335	11294
Unaffected individuals	3	1383

Fisher's exact $p = 3.5 \times 10^{-13}$

	Hotspot consensus position missense DNMs	Other consensus position missense DNMs
ASD probands	19	1868
Unaffected individuals	3	1383

Fisher's exact $p = 0.007$

	Hotspot consensus position missense DNMs	Other consensus position missense DNMs
CHD probands	6	736
Unaffected individuals	3	1383

Fisher's exact $p = 0.07$

Table S9 – Lenient hotspots are significantly enriched for missense variants in NDD and ASD probands

We compared the number of missense DNMs at hotspot positions and other protein consensus positions in cohorts of affected probands (NDD, ASD, and CHD) compared to a set of healthy population controls. NDD and ASD probands have a significant enrichment of missense DNMs in hotspot positions (Fisher's exact test).

	Hotspot consensus position synonymous DNMs	Other consensus position synonymous DNMs
NDD probands	4	3229
Unaffected individuals	0	530

Fisher's exact $p = 1$

	Hotspot consensus position synonymous DNMs	Other consensus position synonymous DNMs
ASD probands	2	717
Unaffected individuals	0	530

Fisher's exact $p = 0.51$

	Hotspot consensus position synonymous DNMs	Other consensus position synonymous DNMs
CHD probands	0	236
Unaffected individuals	0	530

Fisher's exact $p = 1$

Table S10 – Lenient hotspots are not significantly enriched for synonymous variants

We compared the number of synonymous DNMs at hotspot positions and other protein consensus positions in cohorts of affected probands (NDD, ASD, and CHD) compared to a set of healthy population controls. No cohort has a significant enrichment of missense DNMs in hotspot positions (Fisher's exact test).

	Hotspot consensus position unique missense DNMs	Other consensus position unique missense DNMs
ASD probands	13	1821
Unaffected individuals	3	1371

Fisher's exact $p = 0.047$

	Hotspot consensus position unique missense DNMs	Other consensus position unique missense DNMs
CHD probands	0	714
Unaffected individuals	3	1371

Fisher's exact $p = 1$

Table S11 – ASD probands are significantly enriched for unique missense variants at lenient mutation hotspots

We compared the number of unique missense DNMs at hotspot positions and other protein consensus positions in cohorts of affected probands (ASD and CHD) compared to a set of healthy population controls. ASD probands have a significant enrichment of unique missense DNMs in hotspot positions (Fisher's exact test). We defined 'unique DNMs' as those not recurrent in any of the three datasets.

Variant	ACMG classification	Additional Notes
Chr11(GRCh37): g.2432929C>G; ENST00000452833.1; c.2558G>C; p.850R>Q; PF00520:p.102; TRPM5 [MIM *604600]	*Likely Pathogenic (Class 4)*	PS2: De novo (both maternity and paternity confirmed) in a patient with the disease and no family history PM1: Located in a mutational hot spot and/or critical and well-established functional domain (e.g., active site of an enzyme) without benign variation PP3: Multiple lines of computational evidence support a deleterious effect on the gene or gene product (conservation, evolutionary, splicing impact, etc.) HOWEVER: BS1: Allele frequency is greater than expected for disorder
Chr11(GRCh37):g.68848911C>A; ENST00000294309.3; c.1734C>A; p.545R>S; PF00520:p.96; TPCN2 [MIM *612163]	*Likely Pathogenic (Class 4)*	PS2: De novo (both maternity and paternity confirmed) in a patient with the disease and no family history PM1: Located in a mutational hot spot and/or critical and well-established functional domain (e.g., active site of an enzyme) without benign variation PM2: Absent from controls (or at extremely low frequency if recessive) in Exome Sequencing Project, 1000 Genomes Project, or Exome Aggregation Consortium PP3: Multiple lines of computational evidence support a deleterious effect on the gene or gene product (conservation, evolutionary, splicing impact, etc.)
Chr12(GRCh37):g.113706596G>A; ENST00000550785.1 c.963G>A; p.265R>Q; PF00520:p.96; TPCN1 [MIM *609666]	*Likely Pathogenic (Class 4)*	PS2: De novo (both maternity and paternity confirmed) in a patient with the disease and no family history PM1: Located in a mutational hot spot and/or critical and well-established functional domain (e.g., active site of an enzyme) without benign variation PP3: Multiple lines of computational evidence support a deleterious effect on the gene or gene product (conservation, evolutionary, splicing impact, etc.) HOWEVER: BS1: Allele frequency is greater than expected for disorder
Chr14(GRCh37):g.63417240C>T; ENST00000322893.7; c.1249G>A; p.327R>H; PF00520:p.102; KCNH5 [MIM *605716]	*Pathogenic (Class 5)*	PS2 De novo (both maternity and paternity confirmed) in a patient with the disease and no family history PM1: Located in a mutational hot spot and/or critical and well-established functional domain (e.g., active site of an enzyme) without benign variation PM2: Absent from controls (or at extremely low frequency if recessive) in Exome Sequencing Project, 1000 Genomes Project, or Exome Aggregation Consortium PP3: Multiple lines of computational evidence support a deleterious effect on the gene or gene product (conservation, evolutionary, splicing impact, etc.) PP5: Reputable source recently reports variant as pathogenic, but the evidence is not available to the laboratory to perform an independent evaluation
Chr20(GRCh37):g.49621072C>T;EN ST00000371571.4; c.1332G>A; p.349R>H; PF00520:p.102; KCNG1 [MIM *603788]	*Likely Pathogenic (Class 4)*	PS2: De novo (both maternity and paternity confirmed) in a patient with the disease and no family history PM1: Located in a mutational hot spot and/or critical and well-established functional domain (e.g., active site of an enzyme) without benign variation PM2: Absent from controls (or at extremely low frequency if recessive) in Exome Sequencing Project,

		1000 Genomes Project, or Exome Aggregation Consortium PP3: Multiple lines of computational evidence support a deleterious effect on the gene or gene product (conservation, evolutionary, splicing impact, etc.)
Chr9(GRCh37):g.140878675G>A;ENST00000371372.1; *c.1887G>A;* *p.581R>H;* *PF00520:p.102;* *CACNA1B* [MIM *601012]	*Pathogenic (Class 5)*	PS2: De novo (both maternity and paternity confirmed) in a patient with the disease and no family history PM1: Located in a mutational hot spot and/or critical and well-established functional domain (e.g., active site of an enzyme) without benign variation PM2: Absent from controls (or at extremely low frequency if recessive) in Exome Sequencing Project, 1000 Genomes Project, or Exome Aggregation Consortium PP2: Missense variant in a gene that has a low rate of benign missense variation and in which missense variants are a common mechanism of disease PP3: Multiple lines of computational evidence support a deleterious effect on the gene or gene product (conservation, evolutionary, splicing impact, etc.) HOWEVER: 1 occurrence in gnomAD

Table S12 – ACMG classification of DNMs located at stringent hotspots in genes without association to NDDs

Pathogenicity classifications of the variants found at the hotspots that are located in genes that are not in the consensus and discordant gene lists of Kaplanis et al.[4] obtained through variant curation by a laboratory specialist. Abbreviations are according to ACGM[5] guidelines: BS, benign strong; BP, benign supporting; FH, family history; LOF, loss-of-function; MAF, minor allele frequency; path., pathogenic; PM, pathogenic moderate; PP, pathogenic supporting; PS, pathogenic strong; PVS, pathogenic very strong.

Web Resources

YASARA: http://www.yasara.org/
CATH-Gene3D: http://www.cathdb.info/
MetaDome web server: https://stuart.radboudumc.nl/metadome/
MetaDome GitHub repository: https://github.com/cmbi/metadome
RCSB PDB: http://www.rcsb.org

References

1. Samocha, K. E. *et al.* Regional missense constraint improves variant deleteriousness prediction. *bioRxiv* 148353 (2017). doi:10.1101/148353
2. Samocha, K. E. *et al.* A framework for the interpretation of de novo mutation in human disease. *Nat. Genet.* **46**, 944–50 (2014).
3. Karczewski, K. J. *et al.* The ExAC browser: Displaying reference data information from over 60 000 exomes. *Nucleic Acids Res.* **45**, D840–D845 (2017).
4. Kaplanis, J. *et al.* Evidence for 28 genetic disorders discovered by combining healthcare and research data. *Nature* (2020). doi:10.1038/s41586-020-2832-5
5. Richards, S. *et al.* Standards and guidelines for the interpretation of sequence variants: a joint consensus recommendation of the American College of Medical Genetics and Genomics and the Association for Molecular Pathology. *Genet. Med.* **17**, 405–24 (2015).